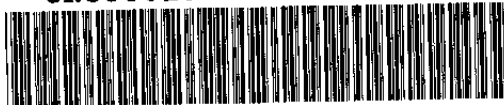


**UNCLASSIFIED**

**AEDC-TR-83-1**

DOC NUM SER CN  
UNC00613-PDC A 1



**Inertial Upper Stage (IUS)**  
**Solid Rocket Motor (SRM)**  
**Core Flow Sampling at High Altitudes**



P. T. Girata, Jr., W. K. McGregor, and R. Quinn  
Sverdrup Technology, Inc.

**November 1983**

**Final Report for Period 1979 – 1982**

Approved for public release; distribution unlimited.

**ARNOLD ENGINEERING DEVELOPMENT CENTER  
ARNOLD AIR FORCE STATION, TENNESSEE  
AIR FORCE SYSTEMS COMMAND  
UNITED STATES AIR FORCE**

**UNCLASSIFIED**

## NOTICES

When U. S. Government drawings, specifications, or other data are used for any purpose other than a definitely related Government procurement operation, the Government thereby incurs no responsibility nor any obligation whatsoever, and the fact that the government may have formulated, furnished, or in any way supplied the said drawings, specifications, or other data, is not to be regarded by implication or otherwise, or in any manner licensing the holder or any other person or corporation, or conveying any rights or permission to manufacture, use, or sell any patented invention that may in any way be related thereto.

Qualified users may obtain copies of this report from the Defense Technical Information Center.

References to named commercial products in this report are not to be considered in any sense as an endorsement of the product by the United States Air Force or the Government.

This report has been reviewed by the Office of Public Affairs (PA) and is releasable to the National Technical Information Service (NTIS). At NTIS, it will be available to the general public, including foreign nations.

## APPROVAL STATEMENT

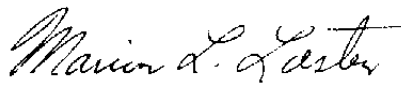
This report has been reviewed and approved.



KENNETH H. LENERS, Captain, USAF  
Directorate of Technology  
Deputy for Operations

Approved for publication:

FOR THE COMMANDER



MARION L. LASTER  
Director of Technology  
Deputy for Operations

## UNCLASSIFIED

SECURITY CLASSIFICATION OF THIS PAGE (When Data Entered)

REPORT DOCUMENTATION PAGE		READ INSTRUCTIONS BEFORE COMPLETING FORM
1. REPORT NUMBER AEDC-TR-83-1	2. GOVT ACCESSION NO.	3. RECIPIENT'S CATALOG NUMBER
4. TITLE (and Subtitle) INERTIAL UPPER STAGE (IUS) SOLID ROCKET MOTOR (SRM) CORE FLOW SAMPLING AT HIGH ALTITUDES		5. TYPE OF REPORT & PERIOD COVERED Final Report - 1979 - 1982
		6. PERFORMING ORG. REPORT NUMBER
7. AUTHOR(s) P. T. Girata, Jr., W. K. McGregor, and R. Quinn, Sverdrup Technology, Inc./ AEDC Group		8. CONTRACT OR GRANT NUMBER(s)
9. PERFORMING ORGANIZATION NAME AND ADDRESS Arnold Engineering Development Center/DOT Air Force Systems Command Arnold Air Force Station, TN 37389		10. PROGRAM ELEMENT, PROJECT, TASK AREA & WORK UNIT NUMBERS Program Elements 62302F and 921E01
11. CONTROLLING OFFICE NAME AND ADDRESS Arnold Engineering Development Center/DOS Air Force Systems Command Arnold Air Force Station, TN 37389		12. REPORT DATE November 1983
14. MONITORING AGENCY NAME & ADDRESS(if different from Controlling Office)		13. NUMBER OF PAGES 35
		15. SECURITY CLASS. (of this report) UNCLASSIFIED
		15a. DECLASSIFICATION/DOWNGRADING SCHEDULE N/A
16. DISTRIBUTION STATEMENT (of this Report) Approved for public release; distribution unlimited.		
17. DISTRIBUTION STATEMENT (of the abstract entered in Block 20, if different from Report)		
18. SUPPLEMENTARY NOTES Available in Defense Technical Information Center (DTIC).		
19. KEY WORDS (Continue on reverse side if necessary and identify by block number) core sampling solid propellant rocket engines particle size gas flow probes		
20. ABSTRACT (Continue on reverse side if necessary and identify by block number) Plume core flow samples which could be analyzed for both gaseous and particle content were obtained during the firing of Inertial Upper Stage (IUS) motors DS4A (Feb. 13, 1981) and DS8C (July 30, 1981) in the AEDC Test Cell J-5 at a simulated altitude of 120 Kft. During the DS4A test, samples were obtained with a tungsten-tipped probe located 10 in. off centerline and 87 in. downstream of the nozzle exit. Three samples were obtained at 1.5, 13.5, and 23.8 sec into the firing. Results of the sampling were generally satis-		

UNCLASSIFIED

SECURITY CLASSIFICATION OF THIS PAGE(When Data Entered)

20. factory, and the probe held up during the sampling period. Analysis of the gas samples gave expected species concentrations. Analysis of the solid material collected revealed that the rocket produced exclusively aluminum oxide with most of the particles less than 2  $\mu\text{m}$  in diameter. Three tungsten-tipped probes were used during the DS8C motor firing. Two probes were located 87 in. downstream, one at the centerline (using water ingestion, 60 g of particles were obtained). The third probe was located 57 in. downstream on the nozzle exit angle. The DS8C analysis compares very well with the DS4A data; all the results are presented in this report.

UNCLASSIFIED

SECURITY CLASSIFICATION OF THIS PAGE(When Data Entered)

## PREFACE

The work reported herein was conducted at the Arnold Engineering Development Center (AEDC), Air Force Systems Command (AFSC), under Program Elements 62302F and 921E01 at the request of the Air Force Rocket Propulsion Laboratory (AFRPL) and the Johnson Space Center (NASA/JSC). The results of the test were obtained by Sverdrup Technology, Inc., AEDC Group, under AEDC Project No. D186EW. Lt. R. Furstenau was the AFRPL Program Manager, Barney Roberts was the NASA Program Manager, and Capt. K. H. Leners was the AEDC Project Manager.

The authors wish to acknowledge the contributions of Mr. Linn Weller of Sverdrup Technology, Inc. (AEDC Group), Mr. Randy Johnson of Pan Am World Services, Inc., (AEDC MSSP), and Mr. R. J. Bryson of Calspan Field Services, Inc. to the success of the program.

## CONTENTS

	<u>Page</u>
<b>1.0 INTRODUCTION .....</b>	<b>5</b>
<b>2.0 CORE FLOW SAMPLING .....</b>	<b>6</b>
<b>2.1 IUS Test Configurations .....</b>	<b>6</b>
<b>2.2 Sampling Technique .....</b>	<b>8</b>
<b>3.0 ANALYSIS TECHNIQUES .....</b>	<b>9</b>
<b>4.0 EXPERIMENTAL RESULTS .....</b>	<b>9</b>
<b>4.1 DS4A Test Data .....</b>	<b>10</b>
<b>4.2 DS8C Test Data .....</b>	<b>11</b>
<b>4.3 Discussion of Sampling Biases .....</b>	<b>13</b>
<b>5.0 SUMMARY OF RESULTS .....</b>	<b>14</b>
<b>REFERENCES .....</b>	<b>16</b>

## ILLUSTRATIONS

### Figure

<b>1. Photograph of IUS Solid Rocket Motor and J-5 Diffuser .....</b>	<b>17</b>
<b>2. Probe Installation for IUS-DS8C Motor in J-5 Test Cell .....</b>	<b>18</b>
<b>3. Schematic of Probe Installation in Diffuser of J-5 Test Cell for Core Flow Sampling of IUS Plume before Firing .....</b>	<b>19</b>
<b>4. Sample Collection System .....</b>	<b>19</b>
<b>5. Location of SEM Stubs in Sample Bottles .....</b>	<b>20</b>
<b>6. Schematic of Water Ingestion Probe .....</b>	<b>20</b>
<b>7. High Magnification Photographs of <math>\text{Al}_2\text{O}_3</math> Particles .....</b>	<b>21</b>
<b>8. SEM Photograph of One Area of Witness Stub from Sample No. 1 with X-Ray Analysis .....</b>	<b>22</b>
<b>9. Histogram of <math>\text{Al}_2\text{O}_3</math> Particles from IUS Motor DS-4A .....</b>	<b>22</b>
<b>10. Photograph and Histogram of IUS-DS8C Centerline Probe — Bottle 1, 1.5 sec, (<math>\text{Al}_2\text{O}_3</math>) .....</b>	<b>23</b>
<b>11. Photograph and Histogram of IUS-DS8C Centerline Probe — Bottle 2, 13.5 sec, (<math>\text{Al}_2\text{O}_3</math>) .....</b>	<b>24</b>
<b>12. Photograph and Histogram of IUS-DS8C Centerline Probe — Bottle 3, 21.5 sec, (<math>\text{Al}_2\text{O}_3</math>) .....</b>	<b>25</b>
<b>13. Histogram of <math>\text{Al}_2\text{O}_3</math> Particles from IUS Motors DS-4A and DS-8C (Centerline Probe) .....</b>	<b>26</b>

<u>Figure</u>	<u>Page</u>
14. Photograph and Histogram of IUS-DS8C Tangent Probe — Bottle 1, 1.5 sec, ( $\text{Al}_2\text{O}_3$ ) .....	27
15. Photograph and Histogram of IUS-DS8C Tangent Probe — Bottle 2, 12.5 sec, ( $\text{Al}_2\text{O}_3$ ) .....	28
16. Photograph and Histogram of IUS-DS8C Tangent Probe — Bottle 3, 21.5 sec, ( $\text{Al}_2\text{O}_3$ ) .....	29
17. Histogram of $\text{Al}_2\text{O}_3$ Particles from IUS Motors DS-4A and DS-8C (Centerline and Tangent Probe) .....	30
18. Photograph and Histogram of IUS-DS8C Tangent Probe — Bottle 1 ( $\text{C}_1$ ) .....	31
19. Photograph and Histogram of IUS-DS8C Tangent Probe — Bottle 2 ( $\text{C}_2$ ) .....	32
20. Photograph and Histogram of IUS-DS8C Tangent Probe — Bottle 3 ( $\text{C}_3$ ) .....	33
21. Photograph and Histogram of IUS-DS8C Water Ingestion Probe ( $\text{Al}_2\text{O}_3$ ) .....	34
22. Histogram of All $\text{Al}_2\text{O}_3$ Particles from IUS Motors DS-4A and DS-8C .....	35

## **TABLES**

1. Predicted Exhaust Species Mole Fractions .....	7
2. Summary of Tests for Particulate Sampling .....	7

## 1.0 INTRODUCTION

During the deployment of space launched systems (e.g., the IUS) from the Space Transportation System (STS), the impact of the solid rocket motor (SRM) plume on mission requirements is of major concern to all users. Potential harmful impacts of the SRM plume are as follows: damage to sensitive orbiter surfaces attributable to SRM plume particle impacts during launch of the payload, and the damage to sensitive space satellite systems attributable to surface contamination of optical windows, solar panels, etc., during orbit insertion.

The sensitive surfaces on the STS are the orbiter viewing windows and the high and low temperature reusable surface insulation (HRSI and LRSI) tiles. The STS damage problem appears in the following forms:

1. Breakage (measured in terms of the number of breaks per unit of surface area).
  - For a window, a break represents the formation of a crater of such a depth ( $40 \mu\text{m}$  or more) that thermal stress during re-entry might induce crack propagation.
  - For a tile, a break represents a penetration of the fused silica coating ( $305\text{-}381 \mu\text{m}$  thick).
2. Erosion (refers to the formation of craters too shallow to be classified as breaks) is measured in terms of the percentage of the total surface area, not depth, that is chipped off by the aggregate of particle impacts.

Assessment of these effects requires knowledge of particle size, flux, and velocity.

The amount of contamination that would damage a sensitive space satellite system is not easily defined. The deposition of condensates and particles on satellite surfaces will degrade the effectiveness of the satellite and ultimately determine its usable life. The allowable amount of deposition requires additional study for a variety of surfaces and contaminants.

To determine the amount of damage to the orbiter caused by particles contained in the aluminized propellant SRM exhaust, a detailed description of particle properties in the SRM plume is required. In the past, various experiments (e.g. Refs. 1 - 3) have been conducted to collect aluminum oxide particle samples to determine their number density and size distribution. The sampling systems were usually biased toward the larger size particles ( $2\text{-}50 \mu\text{m}$ ), and the smaller ( $< 2 \mu\text{m}$ ) particles have been ignored except in a few studies (e.g., Ref.

3). These types of experiments are not adequate for the determination of particle damage to the shuttle or satellite surfaces because of the biased nature of the sample collection systems, and because of the difference in the SRM designs being used in the STS missions from those of previous systems (e.g. Minuteman).

The simulated altitude testing of space application motors in the test cells at AEDC offers a unique opportunity to attempt to characterize the particulates from a variety of rocket motors. Because of its planned usage for STS missions, the IUS propulsion system is of great interest (Ref. 4). An extended development and qualification testing program in the Rocket Development Test Cell (J-5) at AEDC (Ref. 5) offered the opportunity to obtain particulate samples.

The IUS Plume Sampling Program consists of three phases: (1) sampling and analysis of particles contained within the exhaust plume core flow (to assess STS damage); (2) sampling of gas and particulates in the plume boundary region (to evaluate plume back-flow contamination), and (3) sampling of SRM chamber outgassing after completion of the firing. This report deals only with the first of these phases, and the results of the sampling and analysis are given herein.

## 2.0 CORE FLOW SAMPLING

### 2.1 IUS TEST CONFIGURATIONS

The IUS solid rocket motor development program includes a number of altitude tests at AEDC. Two different sizes of IUS motors have been tested: the IUS small motor that has an extendable exit cone (EEC), and the IUS large motor. All core flow samples were taken during two small motor tests in which the carbon-carbon nozzle extended into the diffuser section (Fig. 1).

The main ingredients of the IUS propellant are Hydroxyl Terminated Polybutadiene, Ammonium Perchlorate, and Aluminum (HTPB:AP:AL) in the approximate ratio 13%:68%:18% by weight. The Two-Dimensional Kinetic Nozzle Analysis Computer Program (TDK), Ref. 6, was run at AEDC to predict exhaust products at the exit plane; these products are listed in Table 1. Note that aluminum oxide ( $\text{Al}_2\text{O}_3$ ) makes up about 40 percent by weight of the total equilibrium exhaust products.

**Table 1. Predicted Exhaust Species Mole Fractions**

<chem>Al2O3(S)</chem>	0.087112	HCl	0.151064
CO	0.231450	H <sub>2</sub>	0.366163
CO <sub>2</sub>	0.029856	H <sub>2</sub> O	0.057644
FeCl <sub>2</sub>	0.000033	N <sub>2</sub>	0.076677

Seventy-two additional products were considered, but the mole fractions of these are less than  $0.5 \times 10^{-6}$ .

The probe locations for the two tests are given in Table 2.

**Table 2. Summary of Tests for Particulate Sampling**

IUS Motor	Date Tested	No. of Probes	Location
DS4A	13 February 1981	1	10 in. off centerline 87 in. downstream
DS8C	30 June 1981	3	(1) Centerline, 87 in. downstream  (2) 10 in. off center- line, 87 in. down- stream (water ingestion probe)  (3) Tangent to nozzle exit angle, 51 in. downstream

The 87-in. axial location was chosen such that the probe would be located upstream of the intersection of reflected shocks off the diffuser wall and as far from the nozzle exit as possible to minimize heat transfer. The radial locations were chosen to meet the sponsor's need for determining the spatial variation in the aluminum oxide particle size distribution. Because of a restricted IUS testing schedule, the opportunities were limited to three locations to obtain the core flow data. The tangent location was especially chosen to determine the size distribution of carbon particles that erode from the nozzle surface.

## 2.2 SAMPLING TECHNIQUES

The sampling technique used in acquiring the core flow samples was to locate fixed probes (Fig. 2) at accurately known distances downstream of the nozzle exit at different radial positions. The probe bodies consisted of a 1-in. stainless steel tube surrounded by a carbon steel water jacket which was, in turn, covered with carbon steel plate which served as an ablation coating (Fig. 3). Since the tip of the probe was to be immersed in a high temperature (to 4,000°K) environment with a large concentration of high velocity  $\text{Al}_2\text{O}_3$  particles, a tungsten tip was fabricated and attached to the stainless steel tube sampling line. The probes were considered to be expendable. The water jacket was not intended to cool the outside carbon steel jacket, but was designed to keep the sample tube as cool as possible. The water was turned off before motor burn-out to ensure that water would not be sprayed on the carbon-carbon nozzle. After the firings, the probe hardware located in the core region was found to be severely eroded, but the tungsten tips were not appreciably damaged.

Each core flow probe was connected through the sample transfer line to a sample station. Constant flow through the probe sample lines was maintained by routing a return line back to the diffuser inlet as shown schematically in Fig. 4. Contained in the sample station are three sample bottles of the type shown in Fig. 5. The sample bottles contained a holder for mounting a witness stub to gather particles for analysis using a Scanning Electron Microscope (SEM) combined with an X-ray energy dispersive spectrometer. The 15-mm-diam by 10-mm-thick stubs were made of copper, carbon, or beryllium. Filter paper, used to divide the sample bottle into two compartments (particle/gas), is also held in place by the SEM stub holder as shown in Fig. 5. The gas compartment should then be relatively clear of particles so that the gas can be removed through a line attached to the end opposite the entrance to the sample bottle for gas chromatographic analysis.

The sample station was designed to minimize the number of turns the gas/particle flow has to make before a sample is captured. The sample bottle valves can be operated at any time during the firing and the sample fill time can be selected by use of a sequence controller. The three samples were taken during the first three null periods of the nozzle gimbaling program to ensure sample acquisition at known nozzle positions. Also built into the system for the DS8C motor test was an automatic helium (He) pressurization system which prevented air leakage into the sample bottles between the time the sample was taken and the time the gas analysis was accomplished (about 10 hr).

A large sample of plume particulates (about 100 grams) was collected by modifying the core flow probe to generate a water spray just inside the probe entrance (Fig. 6). This was accomplished by installing 1/4-in. copper tubing inside the probe with a spray head attached to the front end and positioned 3 in. inside the probe entrance. The water ( $\text{H}_2\text{O}$ ) supply

comes from a high pressure tank (1,000 psi) which uses an air operated valve to initiate and terminate the flow. Outside the test cell the probe is connected to a stainless steel collection tank that stores the water/particle slurry. To achieve a pressure in the tank much lower than the pressure at the probe entrance, a vacuum line was installed and positioned just inside the diffuser lip.

### **3.0 ANALYSIS TECHNIQUES**

The gas analysis is not a significant aspect of the orbiter damage problem being addressed in the core flow sampling portion of this effort. This is contrary to the great importance of the gaseous effluents emitted during the postfire period and in the boundary of the plume because of the possibility of condensation of the gaseous species on surfaces. Because of the very high temperature reached by the tungsten tips of the probes and the reactive nature of the gaseous combustion products, it is unlikely that the gas samples, obtained in the core flow, are representative of the rocket exhaust products. Therefore, the gas analysis data are not reported here.

Each sample bottle contained two SEM/X-ray stubs and a filter paper. When the bottles were opened, a visual inspection was completed before the stubs and paper were removed. Sections of the filter paper were cut down to size and mounted on clean SEM/X-ray stubs for analysis. Samples of the water solution that were collected from the water extraction probe were dispersed onto SEM/X-ray stubs for analysis.

The SEM/X-ray unit can define the elemental composition of particulate matter with atomic numbers of 11 (sodium) and greater (see Fig. 7). The SEM/X-ray unit also has an automatic scanning capability that will generate a size histogram of particles 0.25  $\mu\text{m}$  and larger (see Fig. 8).

### **4.0 EXPERIMENTAL RESULTS**

The analysis of the particulate matter found on the SEM stubs and filter paper taken from the sample bottles and water solution is presented in this section. Data presented include photographs of the electron microscope image, size histograms, and X-ray spectral analysis of different areas on the stubs and filters. The procedure used in sampling and data analysis for the two motors, DS4A and DS8C, was sufficiently different to warrant reporting the results separately. Even though the procedures were different, some important observations were made that should be discussed before the test data are presented.

It was observed that all particles (evaluated by the SEM/X-ray unit) were made up of smaller particles (an agglomerate). No matter what particle was being analyzed when the

magnification was increased, the result was an agglomerate of several smaller particles (Fig. 7). This observation is very important when reviewing the histograms presented, since the mechanism of how particles are formed and when they agglomerate has not been conclusively defined.

#### 4.1 DS4A TEST DATA

Only one core flow probe was installed in the diffuser for this test. The sampling times for each bottle were as follows: bottle 1,  $T = +1.5$  sec; bottle 2,  $T = +13.5$  sec, and bottle 3,  $T = 23.8$  sec; 1.5 sec was allowed for sample collection. During sample acquisition, the thrust vector control system was stationary with the nozzle flow aligned with the diffuser. Copper SEM stubs were used in the bottles for this test.

The copper stubs for samples 1 and 3 were analyzed at AEDC using the SEM/X-ray unit. The X-ray analysis of sample 1 (Fig. 8) and sample 3 revealed only particles containing aluminum, assumed to be aluminum oxide,  $\text{Al}_2\text{O}_3$ . Sample 3 X-ray analysis also had traces of stainless steel and tungsten, which leads to the conclusion that the probe had deteriorated by the time this sample was taken.

After the X-ray analysis for both copper stubs was completed, the SEM/X-ray unit was then used to scan for individual particles. Using the automatic scanning capability, particles can be sized and the elemental composition determined. Visual observation of the stubs showed that the particle sizes for sample 1 were predominantly in the range from  $<0.1 \mu\text{m}$  to  $4 \mu\text{m}$ , with only four particles larger than  $4 \mu\text{m}$ . The histogram obtained using the automatic sizing system (lower limit  $0.25 \mu\text{m}$ ) is shown in Fig. 9. All particles included in the analysis were agglomerations of smaller particles and had different shapes; they were not spherical. Sample 3 was completely coated with a grayish material containing some large particles. Upon high magnification, the coating was composed mostly of sub-micron  $\text{Al}_2\text{O}_3$  particles. The large particles ranged from  $50 - 100 \mu\text{m}$  and a few as large as 1 mm were found in the particle collection chamber. X-ray analysis of these large particles showed that they were made of stainless steel and/or tungsten. As stated before, the probe had deteriorated by the time this sample was taken.

The filter paper for both samples was also analyzed to scan for particles to ensure that the procedure for dispersing the particles onto the stub did not bias the sample toward the small particles. The filter paper for sample 1 revealed the same size range as the copper stub (sample 1) as shown in Fig. 9, and the filter for sample 3 was coated with the same grayish material as the copper stub for sample 3.

Analysis of sample bottle 2 was accomplished at the Aerospace Corp. using similar SEM/X-ray equipment. A close spacing of agglomerated smaller particles was found which

was identified as aluminum oxide. No appreciable amounts of other elements were found. The particles were irregular in size and ranged from 0.6 to 10  $\mu\text{m}$ , with an average size of 1.8  $\mu\text{m}$ . A diffraction analysis was also made, and the pattern was found to correspond closely with "alpha"  $\text{Al}_2\text{O}_3$ .

## 4.2 DS8C TEST DATA

For the DS8C test, two core flow probes and the water ingestion probe were installed in the test cell diffuser (Fig. 2). One probe was located 87 in. downstream of the nozzle exit plane and positioned at the centerline. The second probe was located 51 in. downstream of the nozzle exit plane and positioned tangent to the rocket nozzle exit angle. Three samples were acquired from each probe at 1.5, 13.5, and 21.5 sec into the firing. A third probe used to collect a large sample of plume particulates (the water ingestion probe) was located 10 in. off the centerline and positioned 87 in. downstream of the nozzle exit plane. The water ingestion samples were collected continuously from 1.5 sec until 45 sec after ignition. The total motor burn time was 60 sec.

The thrust vector control system was operating during the firing and was stationary at the null position for the 1.5 and 13.5 sec samples. During the sampling at 21.5 sec, the nozzle was stationary but pointed away from the tangent probe at an angle of 4.5 deg with the axis. The centerline probe was thus positioned approximately 13 in. off the nozzle axis for the 21.5 sec sample. The tangent probe position was located between the particle core flow and the plume boundary, as indicated by the sample bottle pressure (44 torr compared to about 10 torr test cell ambient pressure). Thus, the tangent probe should provide a good sample of particles in the boundary layer.

### 4.2.1 Centerline Probe

The sample station used with the centerline probe was modified from that used for motor DS4A to shorten the sample line and add an automatic He pressurization system (see Fig. 4). The He system was required to pressurize the sample bottle to 1 atm to help prevent leakage of air into the sample chamber. The sample bottles are oriented as shown in Fig. 4 and the filling sequence was bottles 1, 2, and 3. The sample bottles contained both carbon and beryllium (Be) stubs for particle analysis. All Be stubs in the sample bottles were severely affected by the HC1 from the exhaust gases; therefore, only the carbon stubs could be used for particle analysis.

The X-ray analysis of the three carbon stubs and filter papers showed primarily  $\text{Al}_2\text{O}_3$  with small traces of tungsten (probe tip). From posttest inspection of the probe and X-ray analysis, it was concluded that the probe did not deteriorate as rapidly as the DS4A probe.

The results of the SEM analysis of the particles collected at the three sampling times are given in Figs. 10 through 12, and a composite histogram of all three samples and the data for motor DSAA are given on Fig. 13. Visual observation of the areas of the stubs analyzed showed particles from less than  $0.1 \mu\text{m}$  to as large as  $5.5 \mu\text{m}$ . Again, the automatic sizing system has a lower limit of  $0.25 \mu\text{m}$  so that the histograms begin at that limit. The majority of the particles sized were in the range  $0.5$  to  $1.5 \mu\text{m}$  with a few larger than  $2 \mu\text{m}$ . Although samples 1 (1.5 sec) and 2 (13.5 sec) were acquired at the centerline and sample 3 (21.5 sec), because of nozzle gimbaling, was acquired 13 in. off centerline, the particle distributions were not very different. In fact, histograms from other areas of a single stub showed as much variation as those for the three samples. Thus the total result should be viewed as a composite (Fig. 13).

#### 4.2.2 Tangent Probe

The sample station for the tangent probe was almost identical to that used for the centerline probe (See Fig. 4). Again, the sample bottles contained both carbon and beryllium stubs for particle analysis. The Be stubs for samples 1 and 2 were severely affected by the HCl, and the Be stub for sample 3 showed no effect. The reason that the Be stubs for 1 and 2 were affected was that the samples were collected from the cove flow where pitot pressure was of the order of 1 atm while for sample 3, the probe was located outside the particle core flow, but in the plume boundary where the pitot pressure was much lower.

Remembering that the X-ray unit used had a lower atomic number limit of 11, particles containing Al ( $A = 13$ ) could be identified, but those containing carbon ( $A = 6$ ) could not. The X-ray analysis of the three carbon and one beryllium stubs and the filter papers revealed only two kinds of particles — those containing  $\text{Al}_2\text{O}_3$  and those giving no identification (assumed to be carbon,  $C_s$ ). One significant difference between the three samples was the ratio of  $\text{Al}_2\text{O}_3$  particles to  $C_s$  particles. Sample bottle 1 showed about 40 percent of the particles to be  $C_s$ ; sample 2 showed about 20 percent, and sample 3 (outside the core flow) showed about 60 percent. No trace of probe material was found in the X-ray analysis. Different areas of the stubs gave similar results.

The  $\text{Al}_2\text{O}_3$  particle size histograms and typical microphotographs of the stubs for the three samples are given in Figs. 14, 15, and 16. The distribution of particles greater than  $0.25 \mu\text{m}$  are similar to those found in the plume center and the histogram of the particles collected outside the core flow (Fig. 16) is only shifted slightly to smaller particles over the core flow sample (Fig. 15). All the histograms are superimposed on Fig. 17, where a composite picture can be seen.

The carbon particle size histograms for the same tangent probe samples are shown in Figs. 18, 19, and 20 for bottles 1, 2, and 3, respectively. Many very small ( $< 0.1 \mu\text{m}$ ) particles

can be detected. All appear to be agglomerations of smaller particles, indicating a sublimation mechanism for removal of the carbon from the nozzle rather than the usual erosion. No carbon particles larger than  $1 \mu\text{m}$  were identified.

#### 4.2.3 Water Ingestion Probe

The water ingestion probe was designed to collect a large sample of plume particulates (about 100 grams), as shown in Fig. 6, by injecting high pressure de-mineralized and filtered water into the probe and creating a shower effect to entrap the particles of the flow. A total of 1.5 gal. of water, which contained the particulate matter, was collected over approximately 44 sec of the burn. Samples were obtained directly from the water by (1) drying droplets on an SEM stub, and (2) extracting particles from the water by using a series of dilution and filtering exercises. The latter process eventually yielded about 45 gm of very pure  $\text{Al}_2\text{O}_3$ . The size histograms for the particles collected by the water ingestion probe are shown in Fig. 21 for both methods of extraction. Little difference is seen in the size distribution for the two methods of extraction. Although particles  $< 0.25 \mu\text{m}$  are observed, there appears to be more agglomeration of the particles collected in this manner.

A composite of all the  $\text{Al}_2\text{O}_3$  size data is given in Fig. 22.

A small sample of the particles collected in the water was also analyzed at the Aerospace Corporation Laboratories. Again, the size distribution was very similar to Fig. 21. However, a more complete X-ray diffraction analysis on the larger sample gave evidence of both alpha and beta crystalline structure of the  $\text{Al}_2\text{O}_3$  particles.

An independent analysis of the large sample of  $\text{Al}_2\text{O}_3$  particles was made by the Grumman Aerospace Corp., Ref. 8, in connection with optical property measurements made in a shock tube. In that study, the particles suspended in the shock heated gas were found to range from 0.1 to  $4.5 \mu\text{m}$ , on the average. Further discussion of them is found in Ref. 8.

### 4.3 DISCUSSION OF SAMPLING BIASES

The main difficulty with all probe sampling techniques is in relating the properties of the sample to the properties in the undisturbed flow. With regard to capturing particle samples from a highly reactive, high temperature, supersonic gas/particle flow, the following biases might be expected:

1. The bow shock created by the probe in the flow would tend to divert smaller particles around the probe, thus biasing the sample collected to larger particles, but the shear forces induced by the shock might also break up the agglomerates.

However, agglomerates might be sheared apart by the stresses created in passing through the shock wave, thus biasing toward smaller particles.

2. Adherence of material to the probe inlet and sample line would appear to favor smaller particles, again biasing the sample to larger particles. However, a careful cleaning of the sample lines for the tangent probe did not reveal any large particles, either  $\text{Al}_2\text{O}_3$  or carbon.
3. Sharp turns into the sampling bottles would tend to bias the sample toward smaller particles — the larger ones striking the walls and either breaking up or adhering to the walls. However, sample bottle 3 was connected so that the flow was straight into the bottle and no appreciable change in the particle distribution was noted over samples 1 and 2 (See Figs. 10, 11, and 12).
4. Impact of agglomerated particles on surfaces near the probe inlet would tend to break the cluster into smaller particles, thus biasing the sample toward the smaller particles. These particles, however, would probably be swept around the probe in the reaccelerating flow.
5. Particles striking the witness stubs inside the sample bottles might either break up or bounce off the surface, again possibly biasing the sample toward smaller particles. However, the size distribution of the particles found on the filter paper was not appreciably different from that of the SEM stubs.

All these possibilities were considered during this study and are worthy of further investigation. However, such a study would be difficult because of the necessity to use particles made up of agglomerations of the smaller, more fundamental  $\text{Al}_2\text{O}_3$  particles. Such particles are found only in the products of combustion of aluminum. The fact that essentially the same size distribution of particles was found in each bottle, regardless of orientation, and in the water ingestion sample tends to imply that items 2 through 5 are not very important considerations. Thus, there is reason to believe that the particle samples are relatively unbiased by the sampling technique, except for the possible breakup during passage through the bow shock in front of the probe. Further study of this phenomenon is warranted.

## 5.0 SUMMARY OF RESULTS

The results obtained in this study of the particle emission from IUS rocket exhausts may be summarized as follows:

1. The method of sampling by the use of tungsten-tipped probes with a carbon steel ablation protected stainless steel sample transfer line leading to sample

bottles equipped with particle witness stubs proved to be an effective means to gather samples from solid rocket motor exhausts.

2. Within the core flow region of the exhaust plume of IUS motors, only  $\text{Al}_2\text{O}_3$  solid particles were found. Under scanning electron microscope observation, the particles were found to consist of very fine unit particles (less than  $0.1 \mu\text{m}$ ) which agglomerated to form larger particles. Very few agglomerations greater than  $2 - 3 \mu\text{m}$  were found.
3. In the boundary region tangent to the nozzle exit angle (just inside visible coreflow), the particulate samples were made up of about 60 to 80 percent  $\text{Al}_2\text{O}_3$  and 20 to 40 percent solid carbon,  $\text{C}_s$ . The size distribution of the  $\text{Al}_2\text{O}_3$  particles was very nearly the same as for the inner core. The largest  $\text{C}_s$  particles were  $0.5 \mu\text{m}$  with most of them less than  $0.25 \mu\text{m}$ .
4. Particulates were also found in the boundary region between the core flow (tangent to nozzle exit) and the underexpanded plume boundary. The particles were a mixture of  $\text{Al}_2\text{O}_3$  and  $\text{C}_s$  in about a 40 percent/60 percent ratio. The size distribution was approximately the same as found in the inner core near the boundary, but the density of particles collected was much less.
5. Particles collected in a water ingestion sample did not appreciably differ in size from the dry sampling method.
6. No conclusive reasons have been found to indicate a biasing of the particle sizes by the sample handling procedure, but breakup within the probe bow shock cannot be ruled out as a possibility.

These results affect the analysis of the orbiter damage assessment in that the impact damage from large particles may be ignored. However, the erosion effect from many small particles must still be considered. Moreover, it appears that there is no preferred orientation of the IUS thrust axis with the orbiter position with respect to particle size. The flux of particles as a function of plume radius has, however, not been determined.

It is not possible to generalize these results to other SRM configurations. The carbon-carbon nozzle used in the IUS motors evidently does not permit condensation of  $\text{Al}_2\text{O}_3$  in the throat region, since it is clean and uniform after the firing with no apparent  $\text{Al}_2\text{O}_3$  deposits. The larger particles observed previously from Minuteman class motors using ablative nozzles are possibly the result of this wall effect. It is thus recommended that sampling of the exhausts of other SRM's of interest be undertaken before general conclusions are drawn.

## REFERENCES

1. Geisler, R. L., Beckman, C. W., Kinkead, S. A. "The Relationship Between Solid Propellant Formulation Variables and Motor Performance." AIAA Paper No. 25-1199, October 1975.
2. Hermsen, R. W. "Aluminum Oxide Particle Size for Solid Rocket Motor Performance Prediction." AIAA Paper No. 81-0035, January 1981.
3. Dawbarn, R. and Kinslow, M. "Studies of the Exhaust Products from Solid Propellant Rocket Motors." AEDC-TR-76-49 (AD-A029569), September 1976.
4. McDonnell Douglas Technical Services Corporation. "Orbiter Surface Damage Due to SRM Plume Impingement." TM-1.4-MAB-314, March 30, 1979.
5. *Test Facilities Handbook* (Eleventh Edition). "Engine Test Facility, Vol. 2." Arnold Engineering Development Center, April 1981.
6. Ultrasystems, Inc. "Engineering and Programming Manual Two-Dimensional Kinetic (TDK) Reference Computer Program." NASA-CR-152999, December 1973.
7. Konopka, W., Reed, R. A., Calia, V. S. "Infrared Optical Properties of  $\text{Al}_2\text{O}_3$  IUS Motor (DS8C) Exhaust Particles." AEDC-TR-83-19, April 1983.

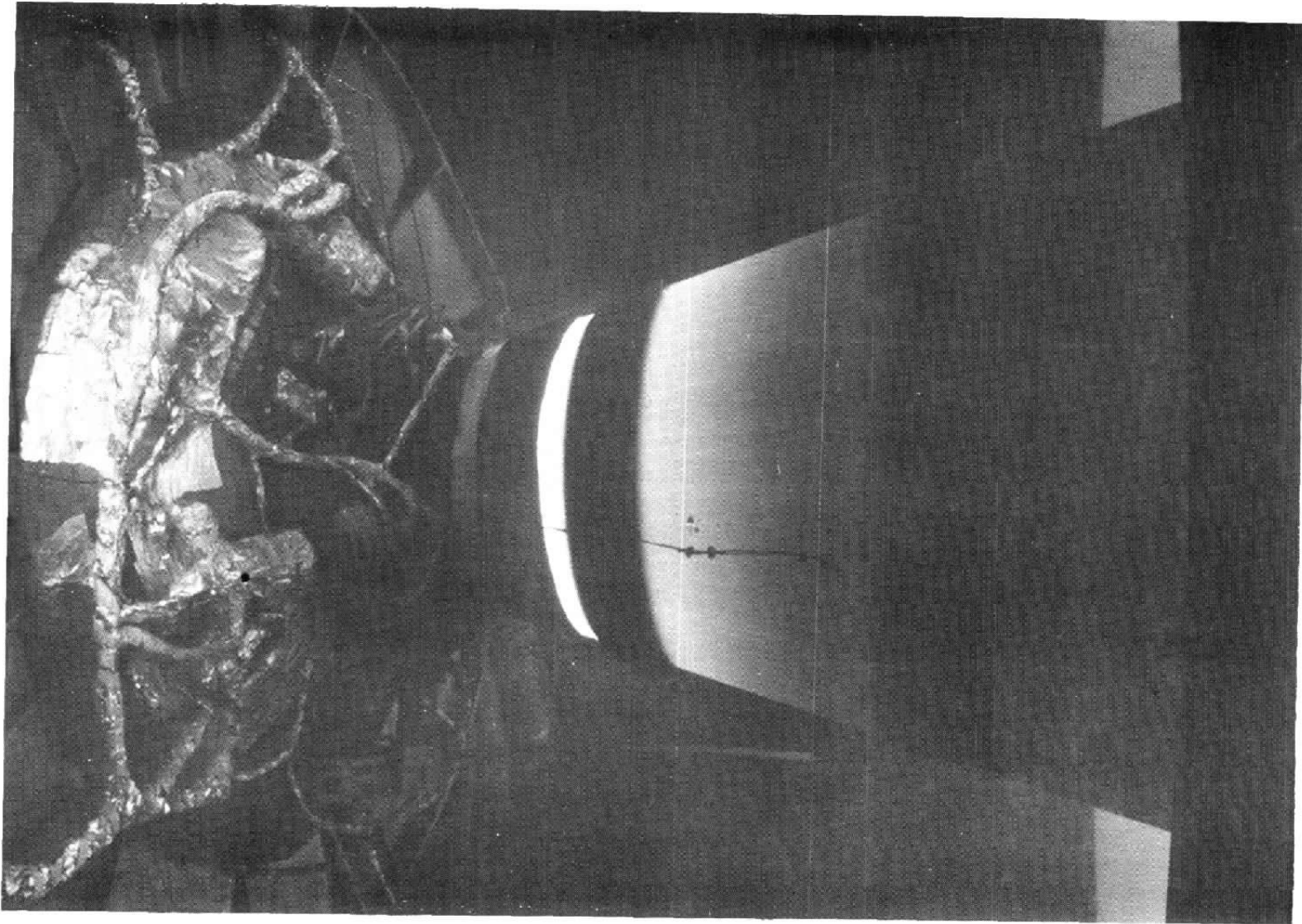


**Figure 1. Photograph of IUS solid rocket motor and J-5 diffuser.**

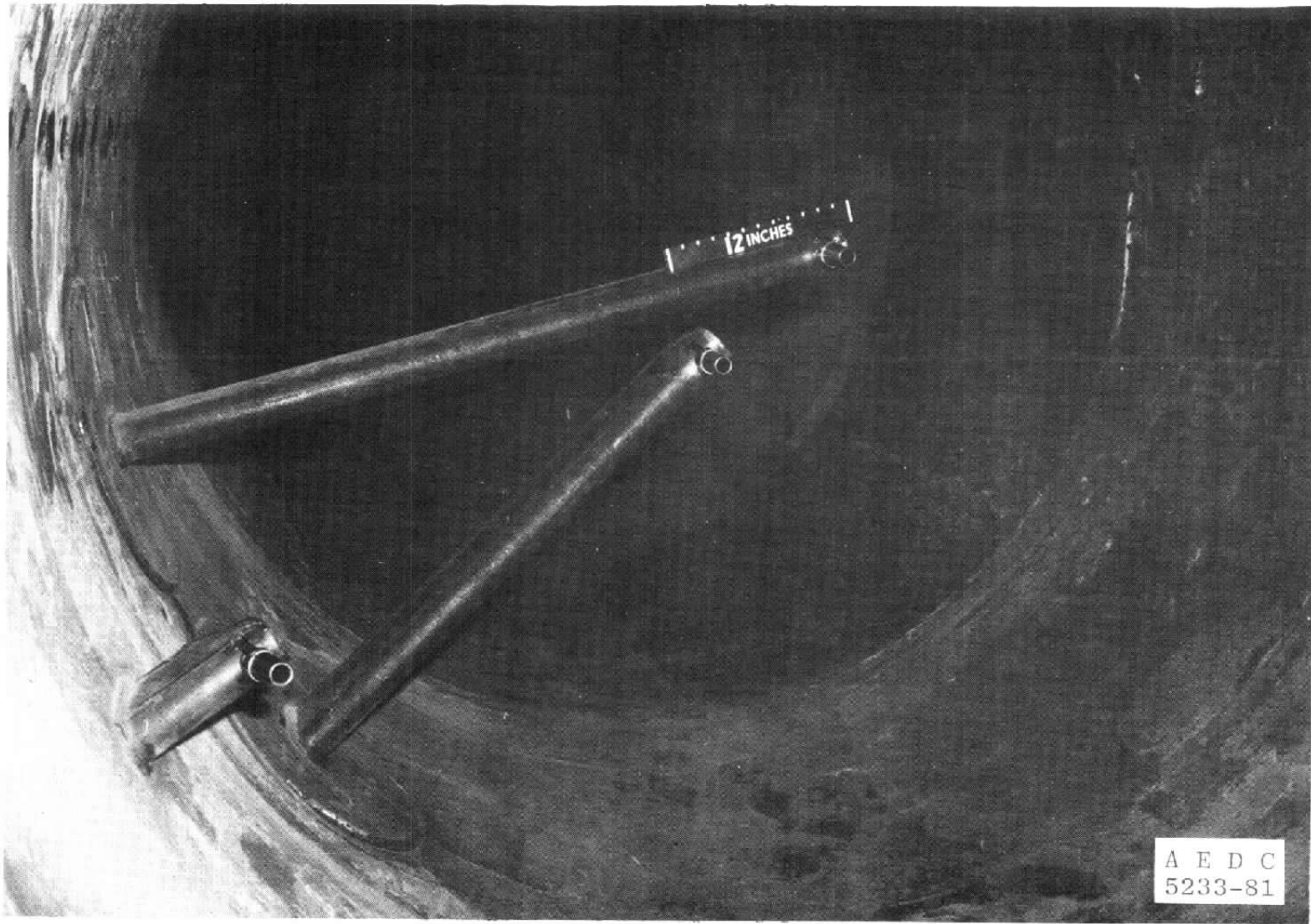


**Figure 2. Probe installation for IUS-DS8C motor in J-5 test cell.**

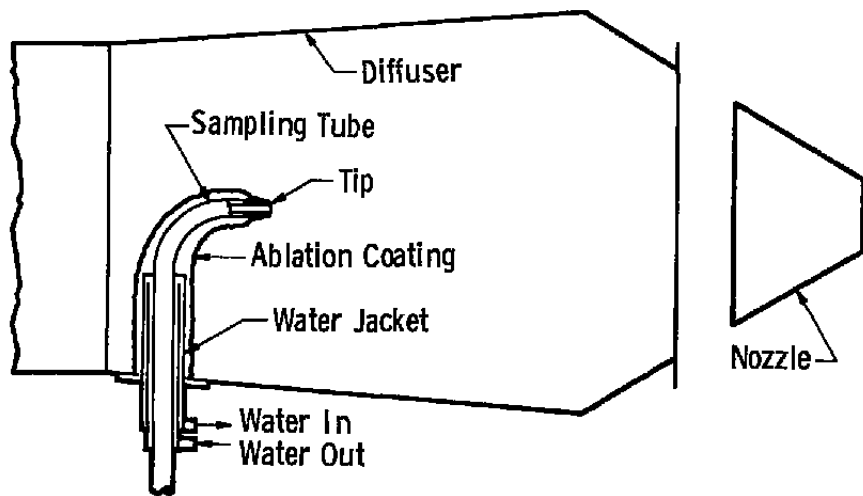


**Figure 3. Schematic of probe installation in diffuser of J-5 test cell for core flow sampling of IUS plume before firing.**

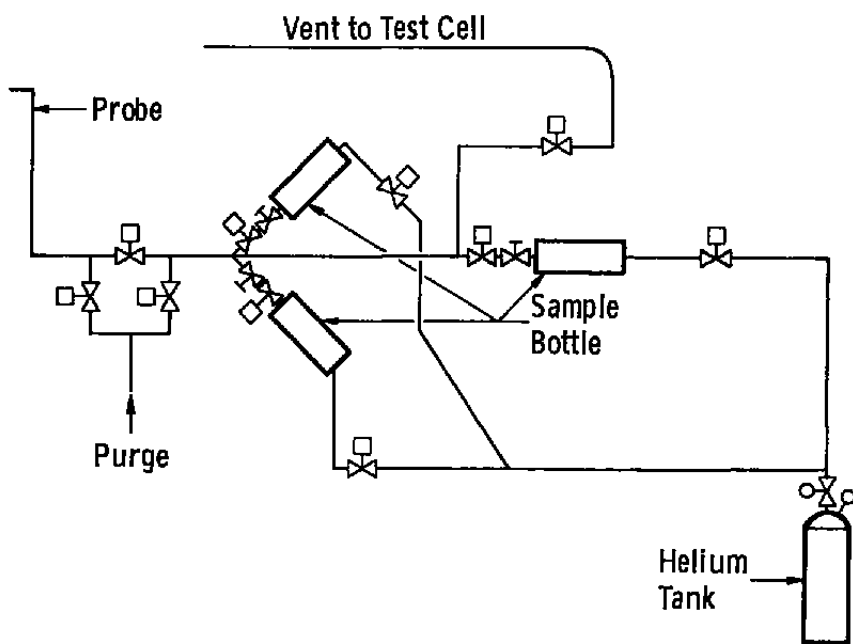


**Figure 4. Sample collection system.**

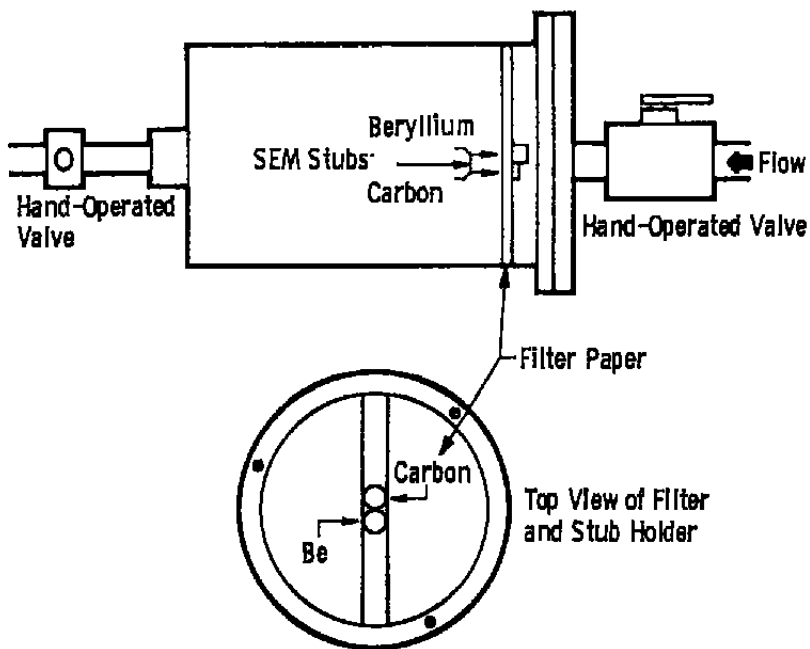


**Figure 5. Location of SEM stubs in sample bottles.**

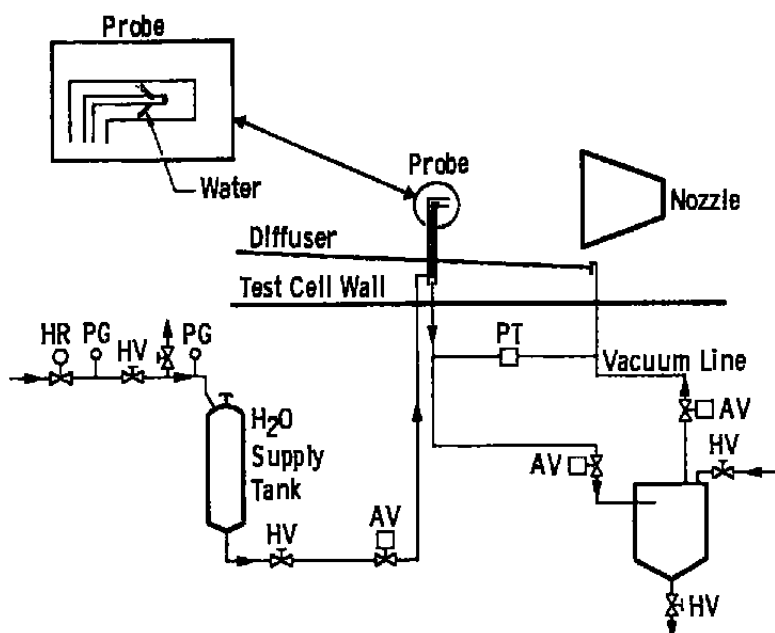
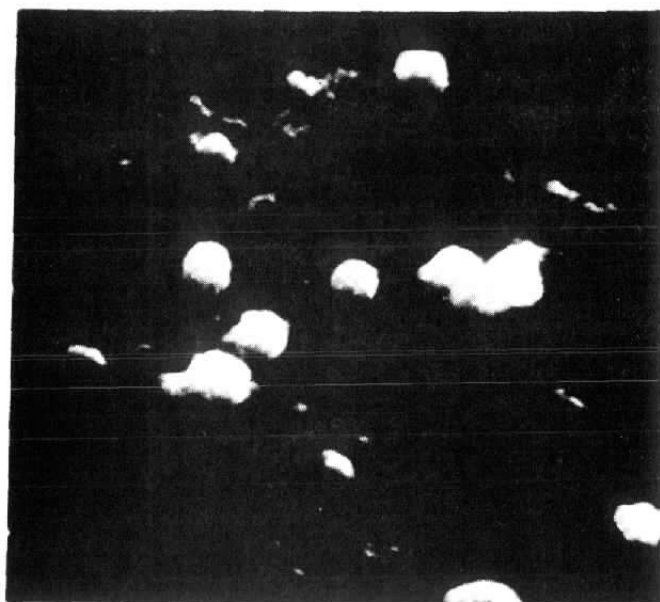
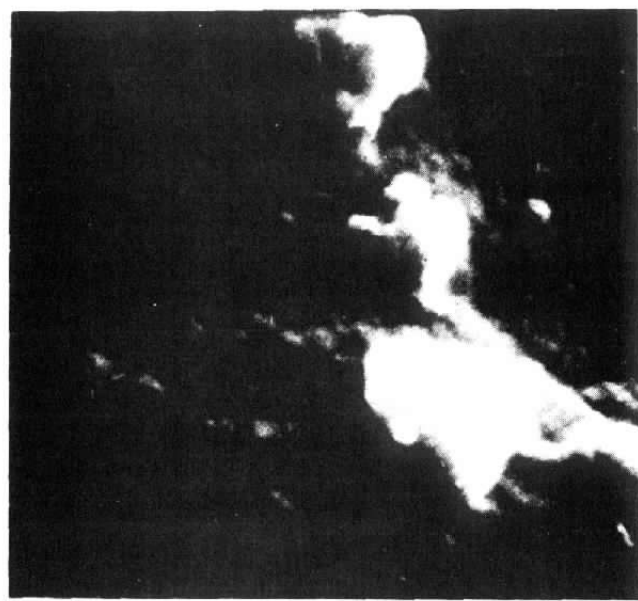


**Figure 6. Schematic of water ingestion probe.**

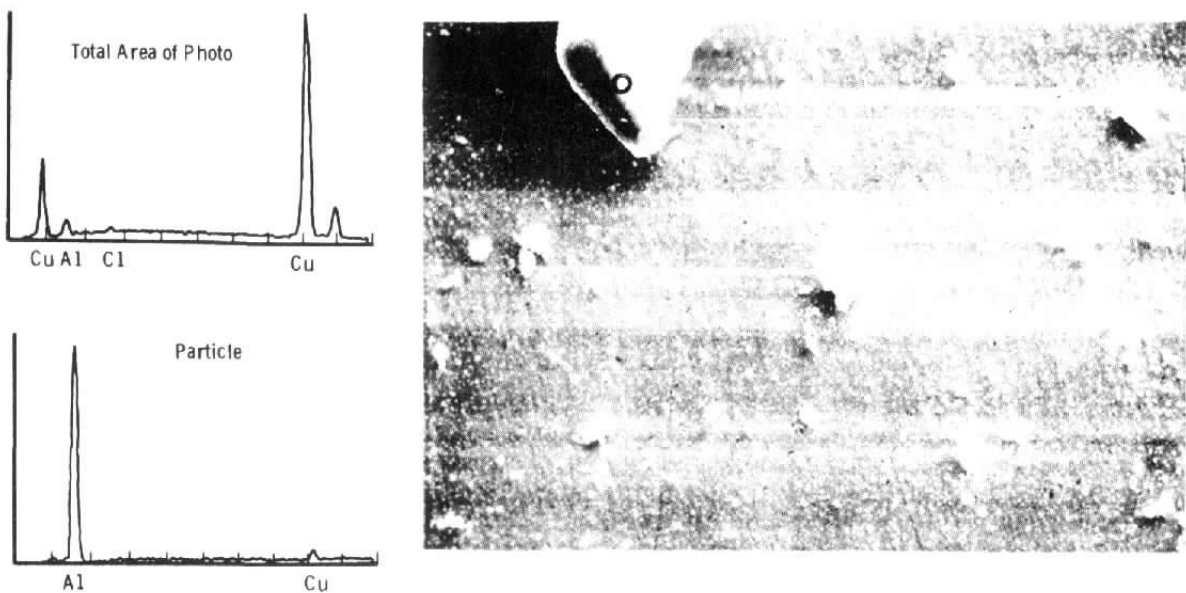


a. 24,000 X

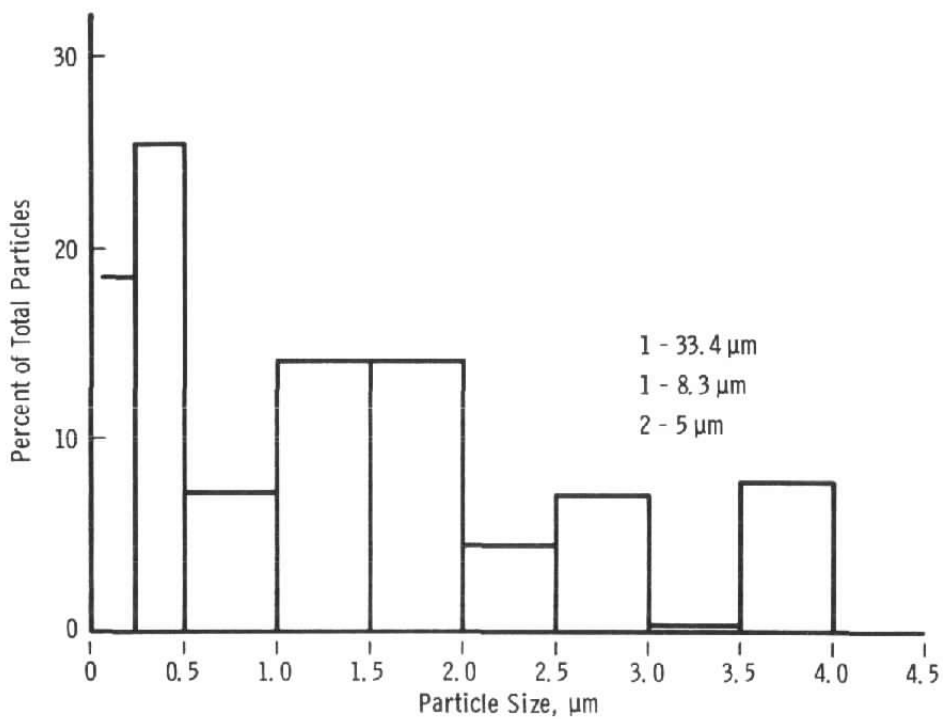


b. 36,000 X

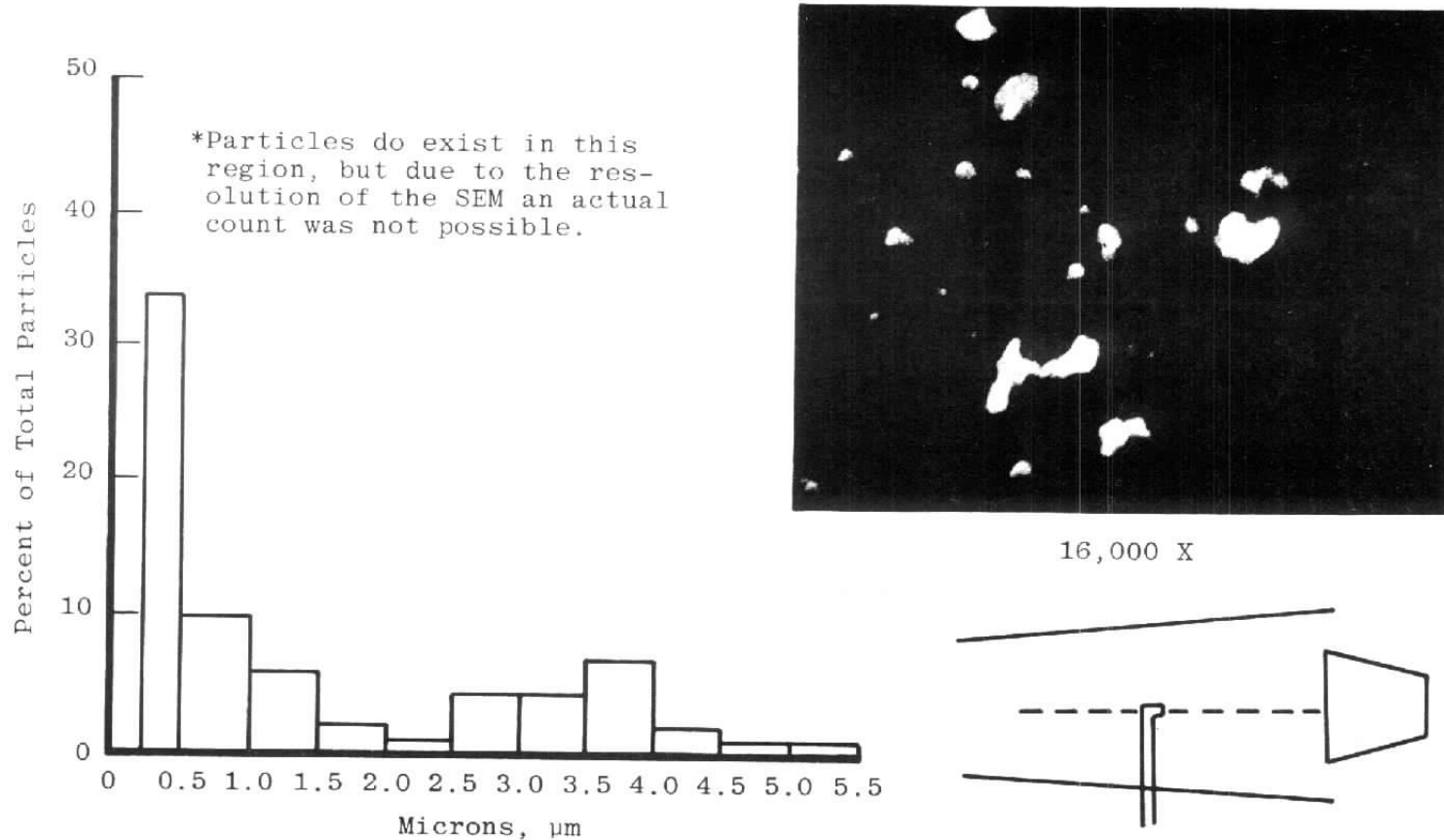
**Figure 7. High magnification photographs of  $\text{Al}_2\text{O}_3$  particles.**



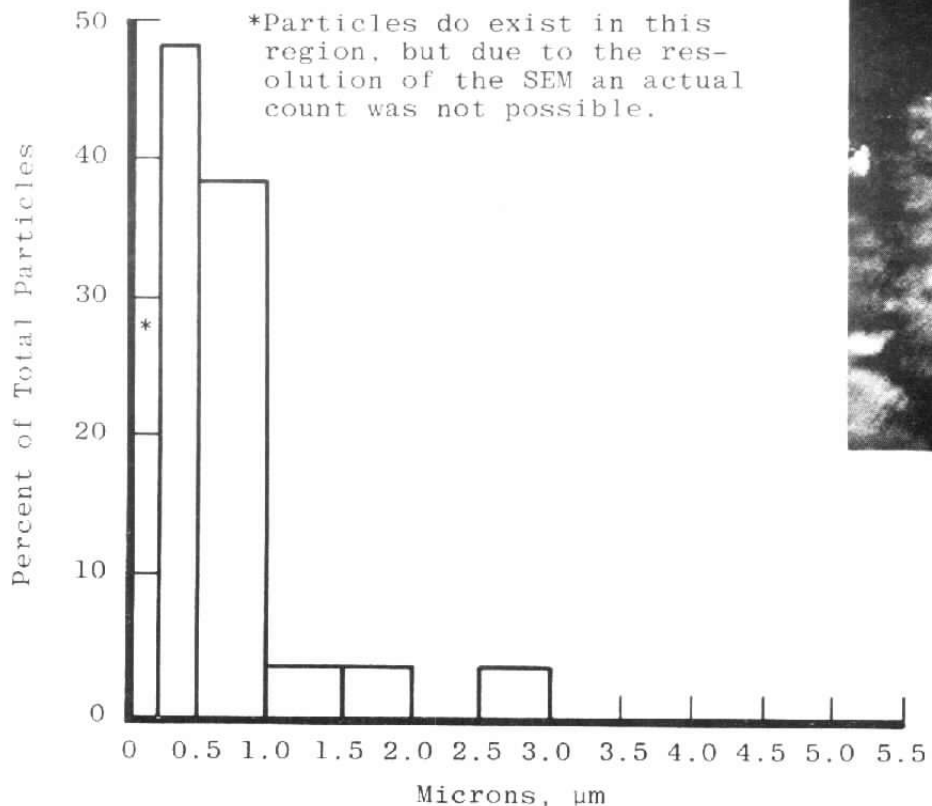
**Figure 8. SEM photograph of one area of witness stub from sample No. 1 with X-ray analysis.**



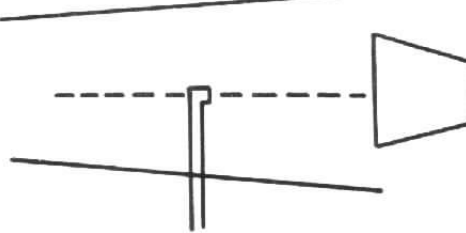
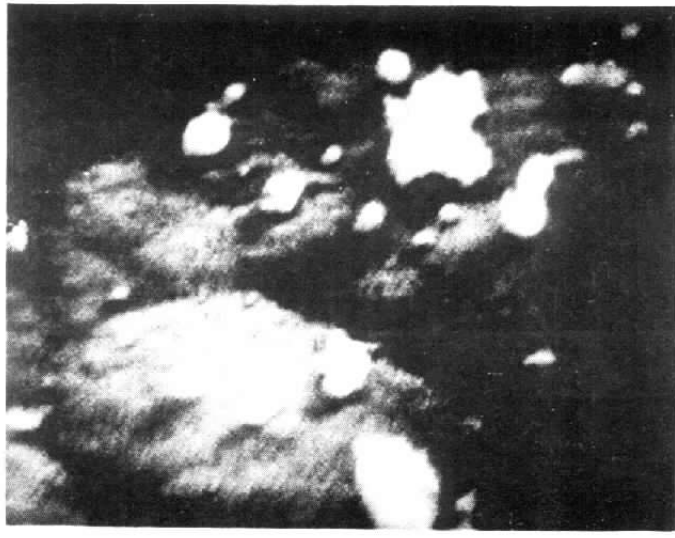
**Figure 9. Histogram of  $\text{Al}_2\text{O}_3$  particles from IUS Motor DS-4A.**

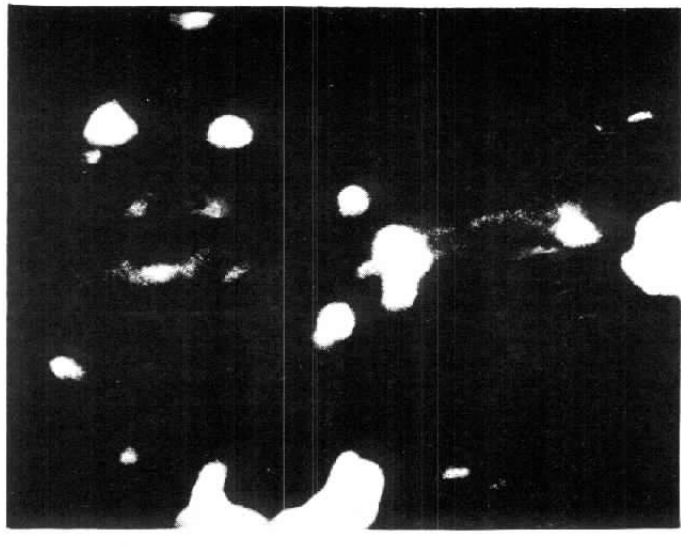
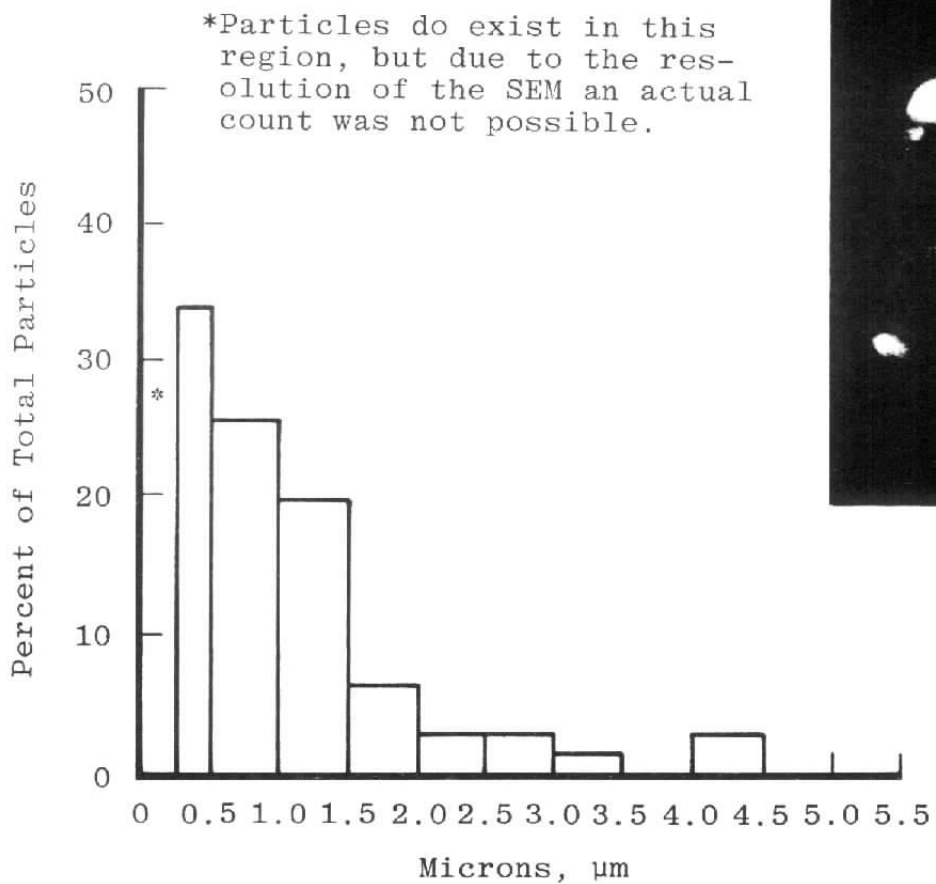


**Figure 10. Photograph and histogram of IUS-DS8C centerline probe — Bottle 1,  
1.5 sec, ( $\text{Al}_2\text{O}_3$ ).**



**Figure 11. Photograph and histogram of IUS-DS8C centerline probe — Bottle 2,  
13.5 sec, ( $\text{Al}_2\text{O}_3$ ).**





12,000 X

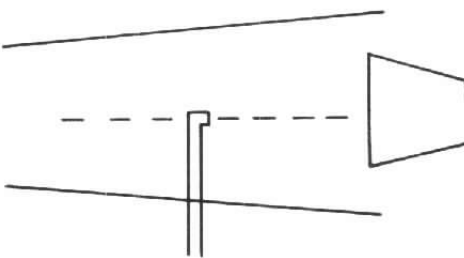


**Figure 12. Photograph and histogram of IUS-DS8C centerline probe — Bottle 3,  
21.5 sec, ( $\text{Al}_2\text{O}_3$ ).**

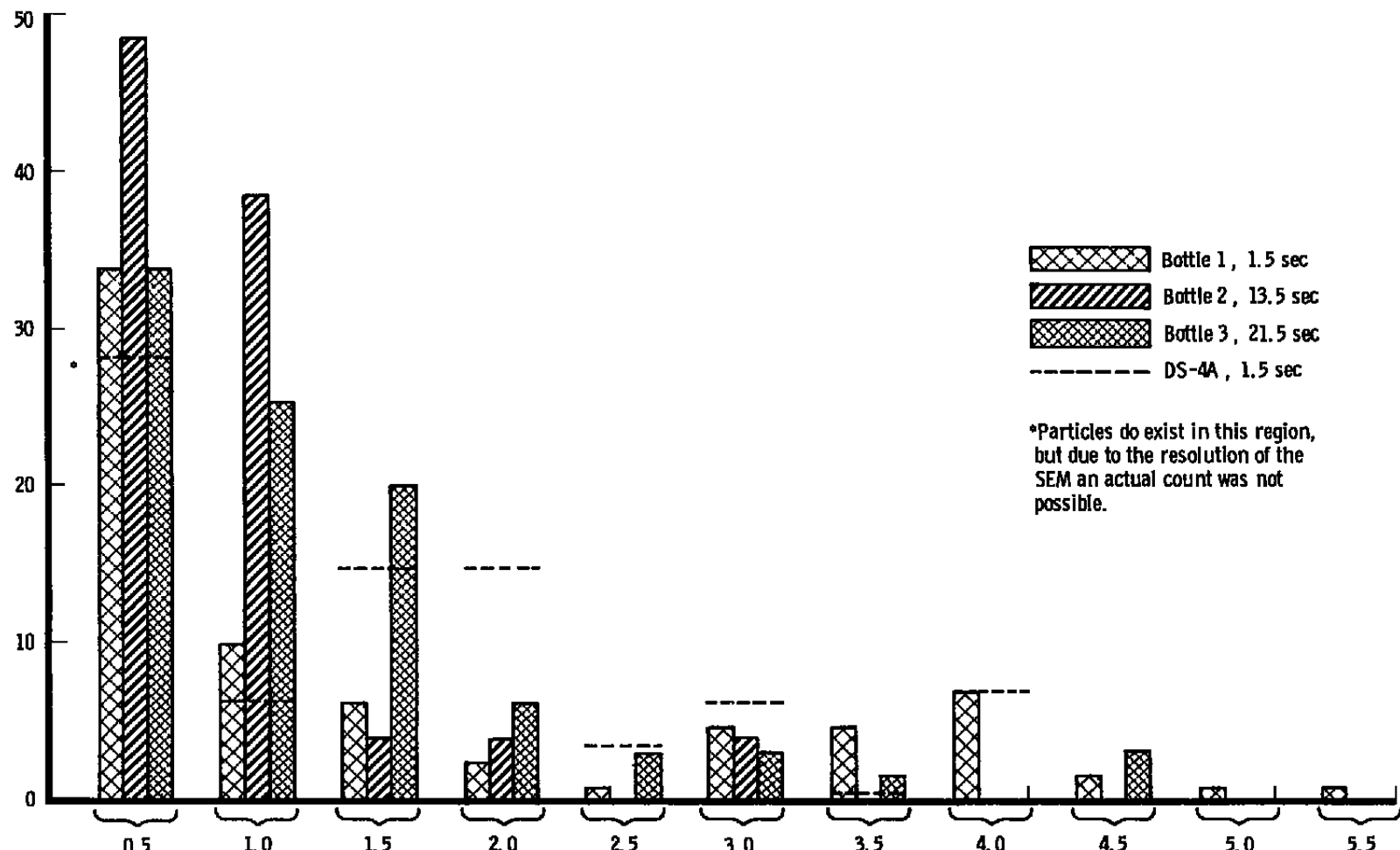
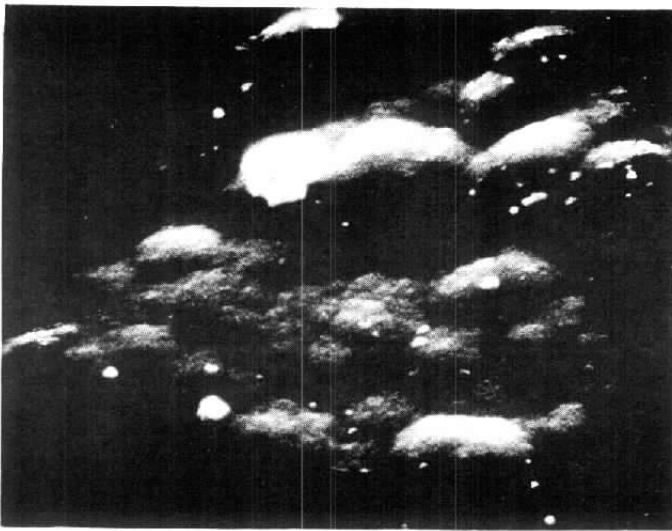
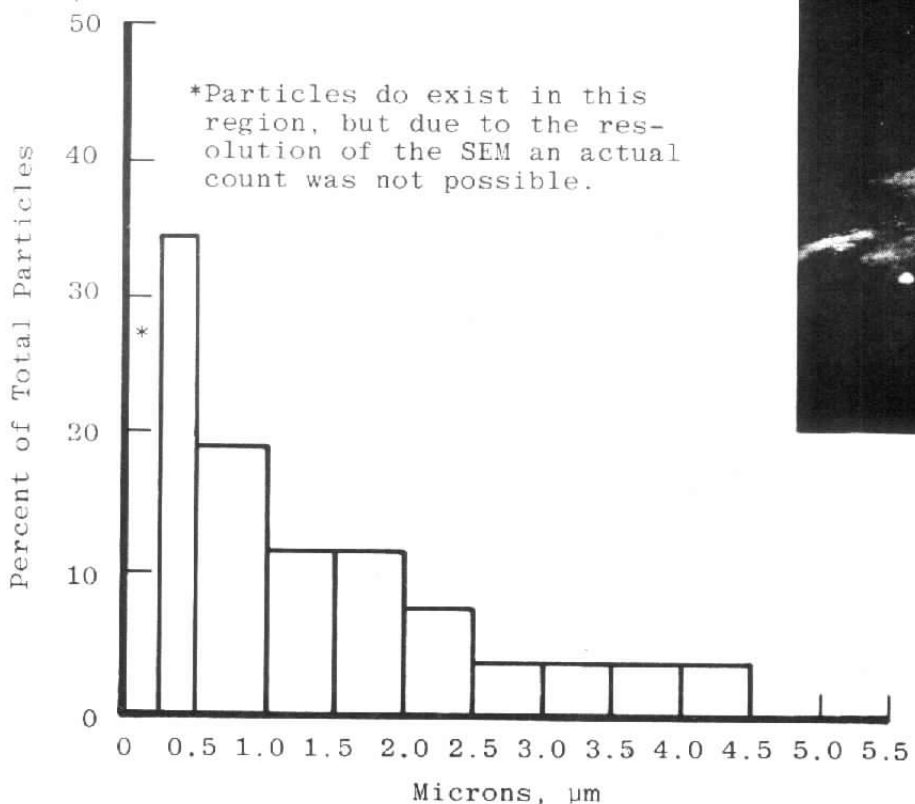
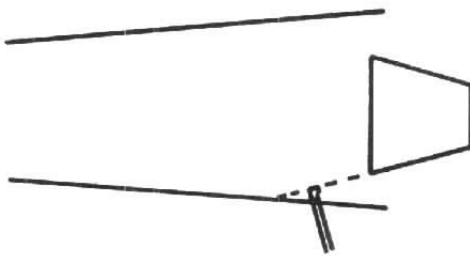


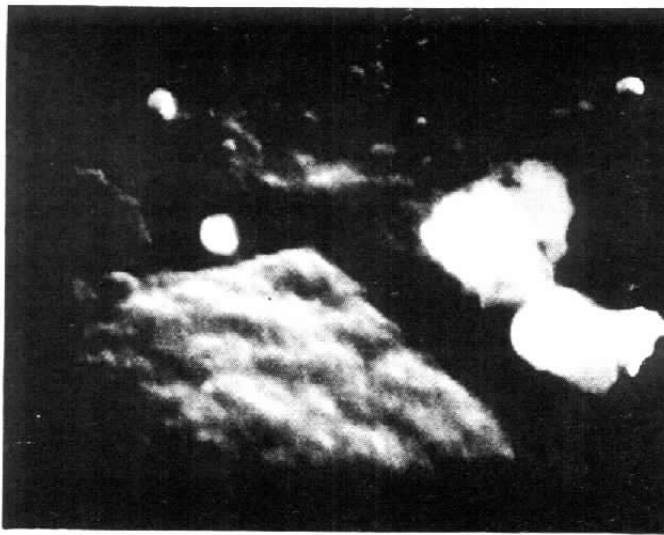
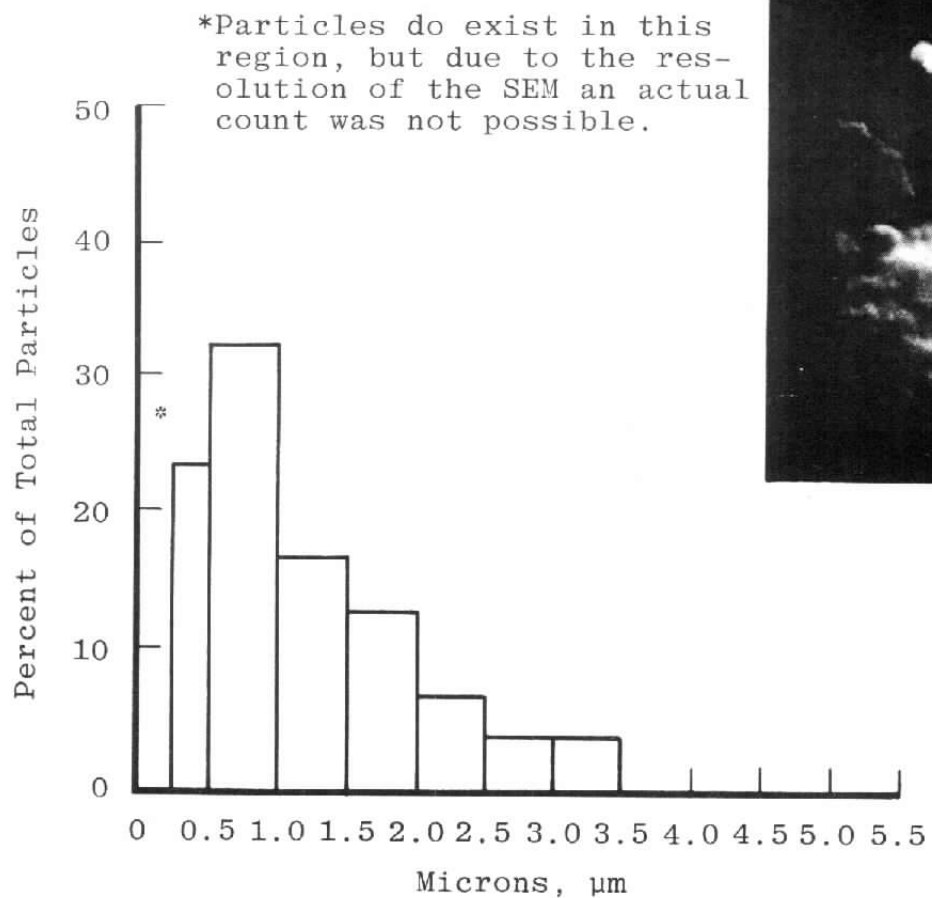
Figure 13. Histogram of  $\text{Al}_2\text{O}_3$  particles from IUS Motors DS-4A and DS-8C (centerline probe).



3,000 X



**Figure 14. Photograph and histogram of IUS-DS8C tangent probe — Bottle 1, 1.5 sec, ( $\text{Al}_2\text{O}_3$ ).**



18,000 X

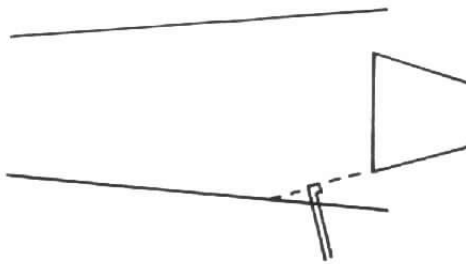


**Figure 15. Photograph and histogram of IUS-DS8C tangent probe — Bottle 2,  
13.5 sec, ( $\text{Al}_2\text{O}_3$ ).**

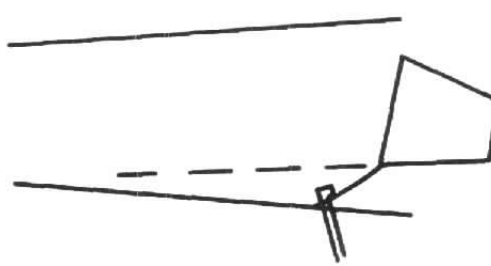
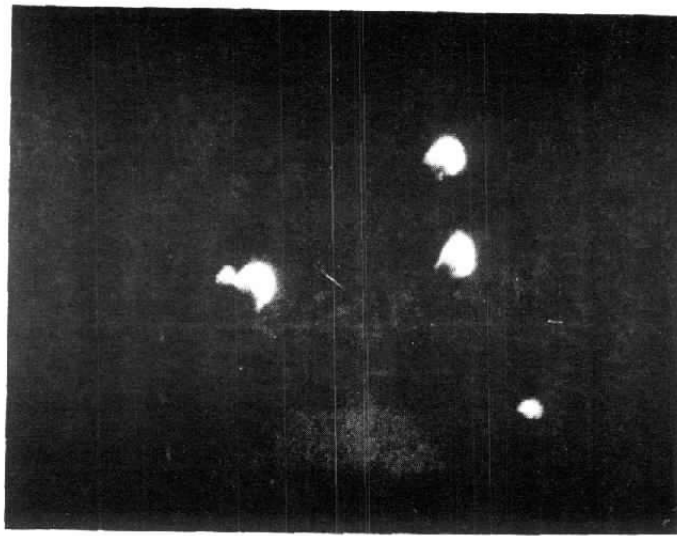
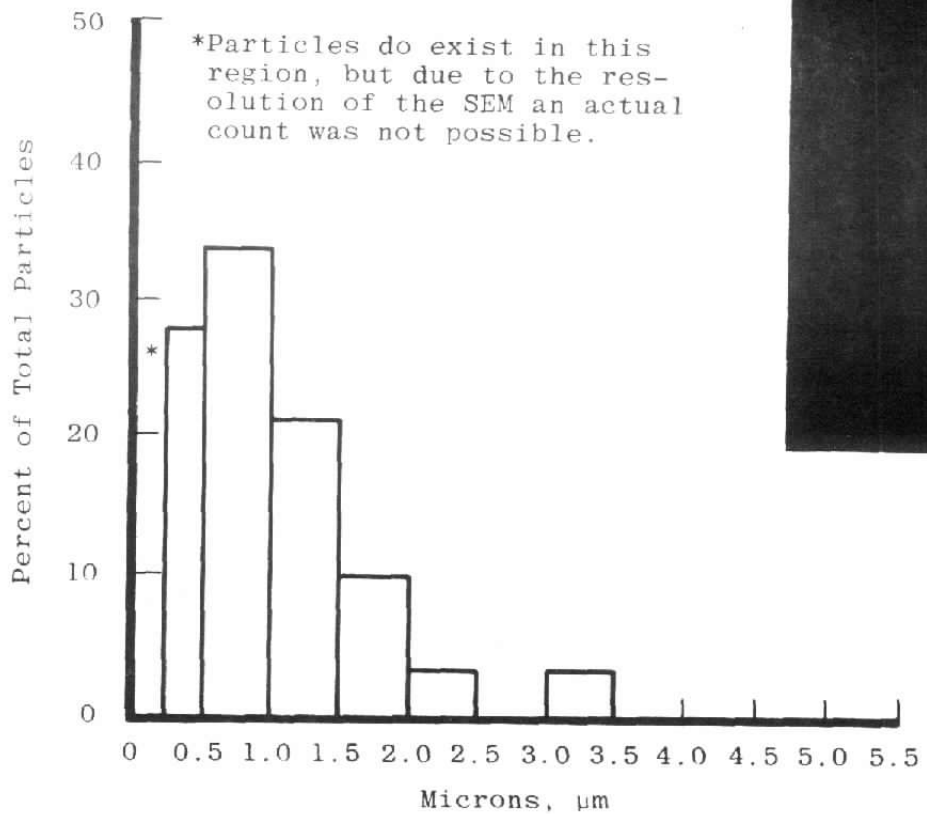


**Figure 16. Photograph and histogram of IUS-DS8C tangent probe — Bottle 3,  
21.5 sec, ( $\text{Al}_2\text{O}_3$ ).**

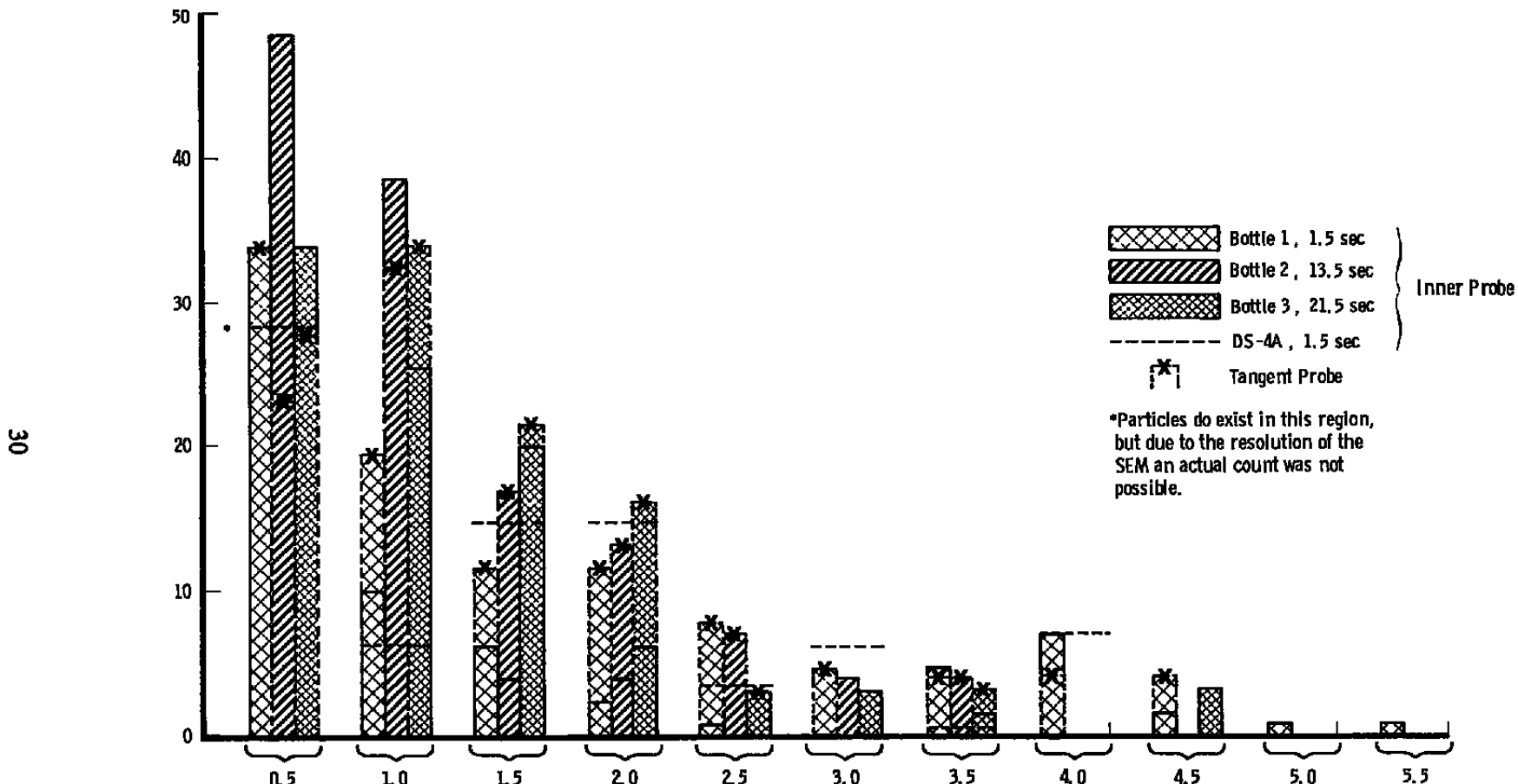
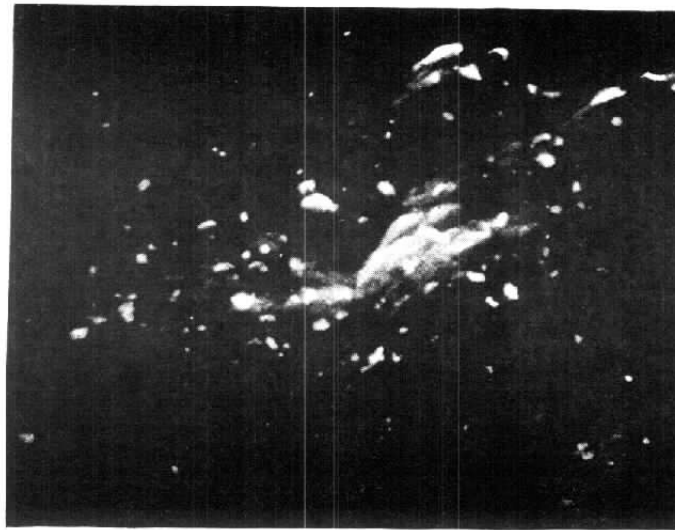
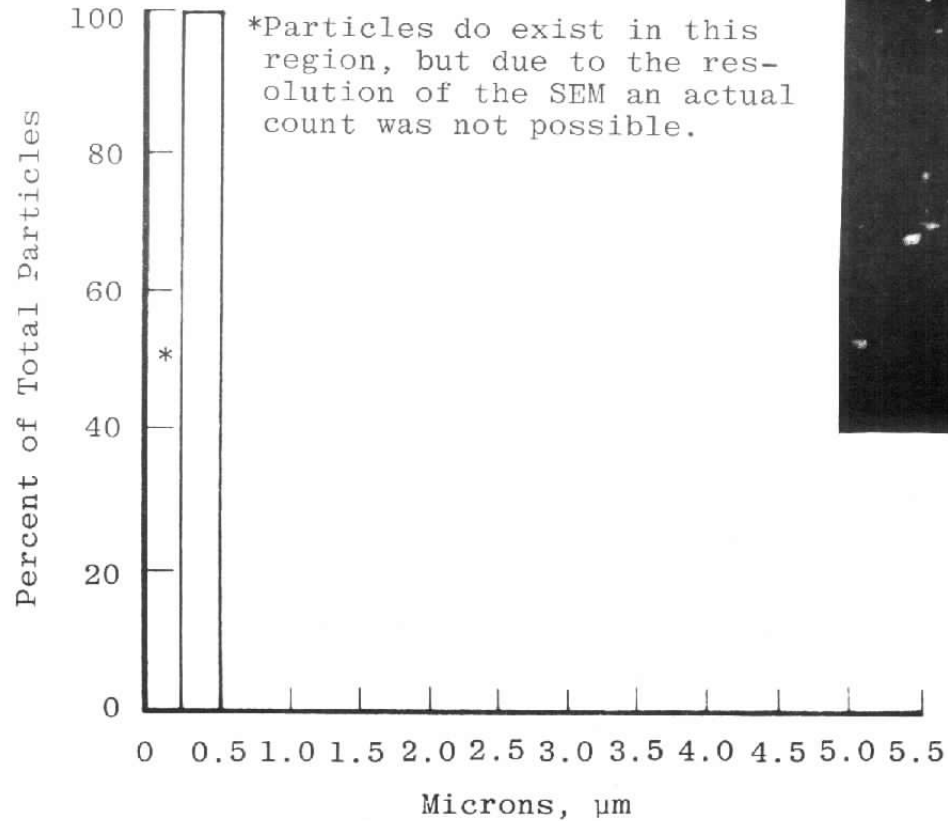
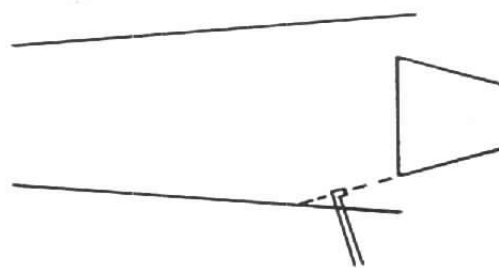


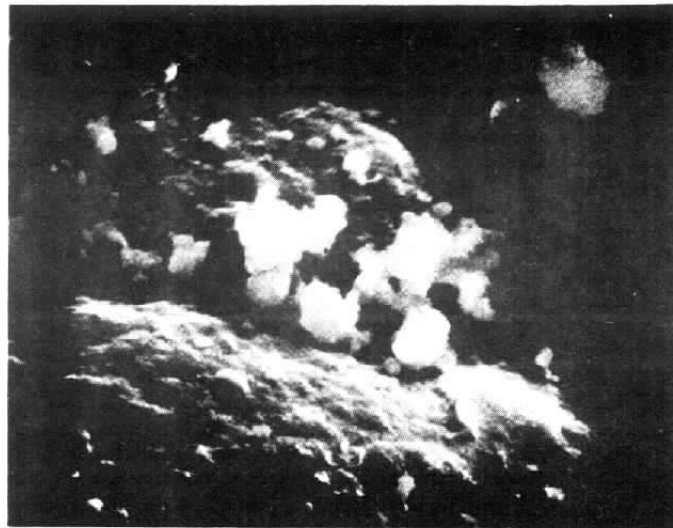
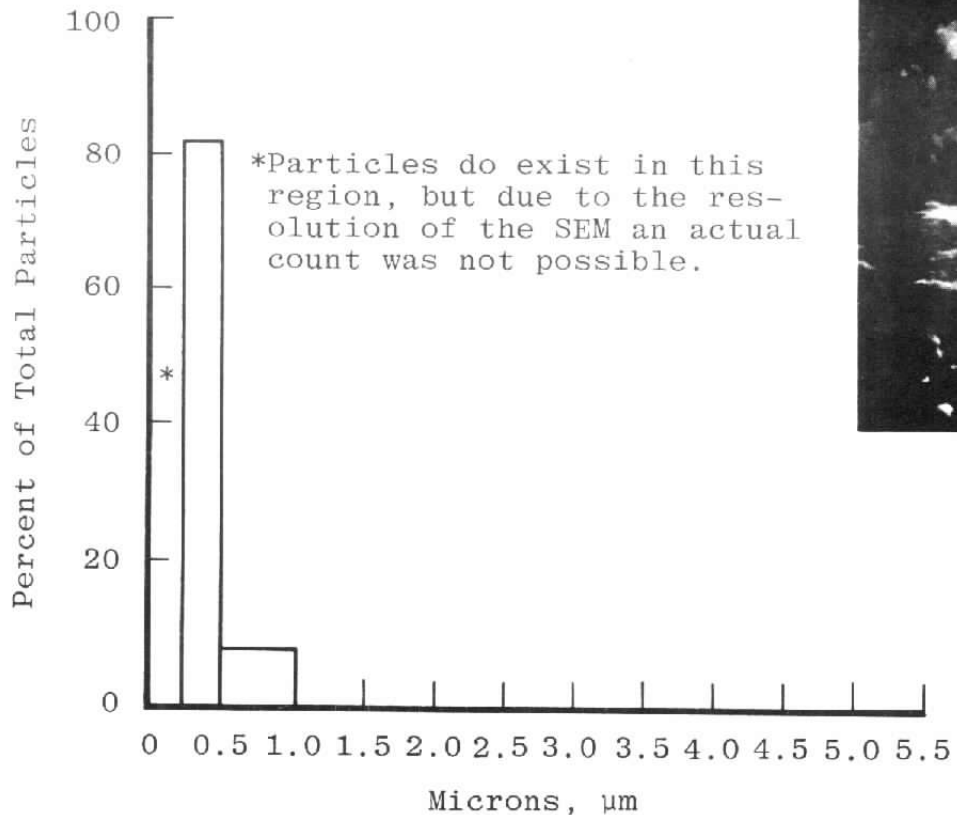
Figure 17. Histogram of  $\text{Al}_2\text{O}_3$  particles from IUS motors DS-4A and DS-8C (centerline and tangent probe).



3,000 X



**Figure 18. Photograph and histogram of IUS-DS8C tangent probe — Bottle 1 ( $C_s$ ).**



9,000 X

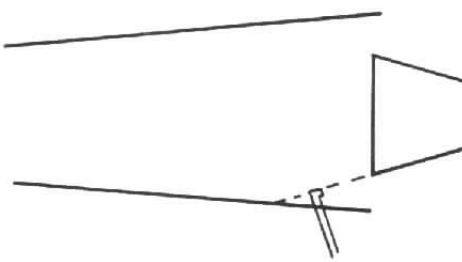


**Figure 19. Photograph and histogram of IUS-DS8C tangent probe — Bottle 2 ( $C_s$ ).**

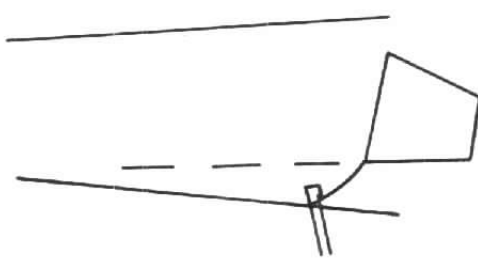
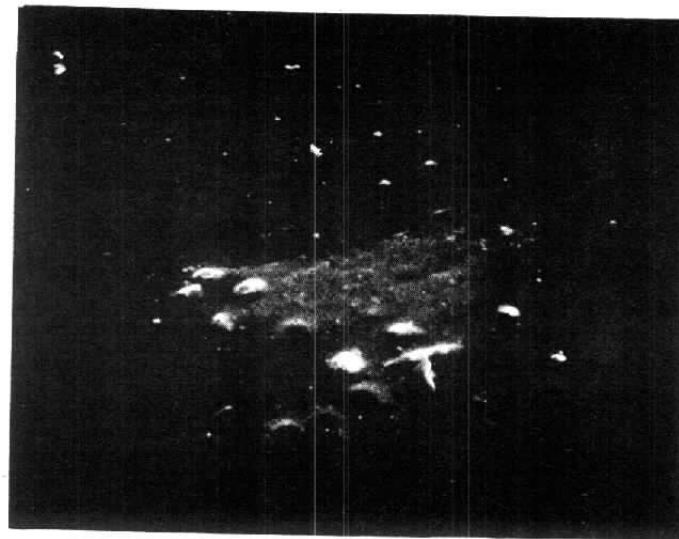
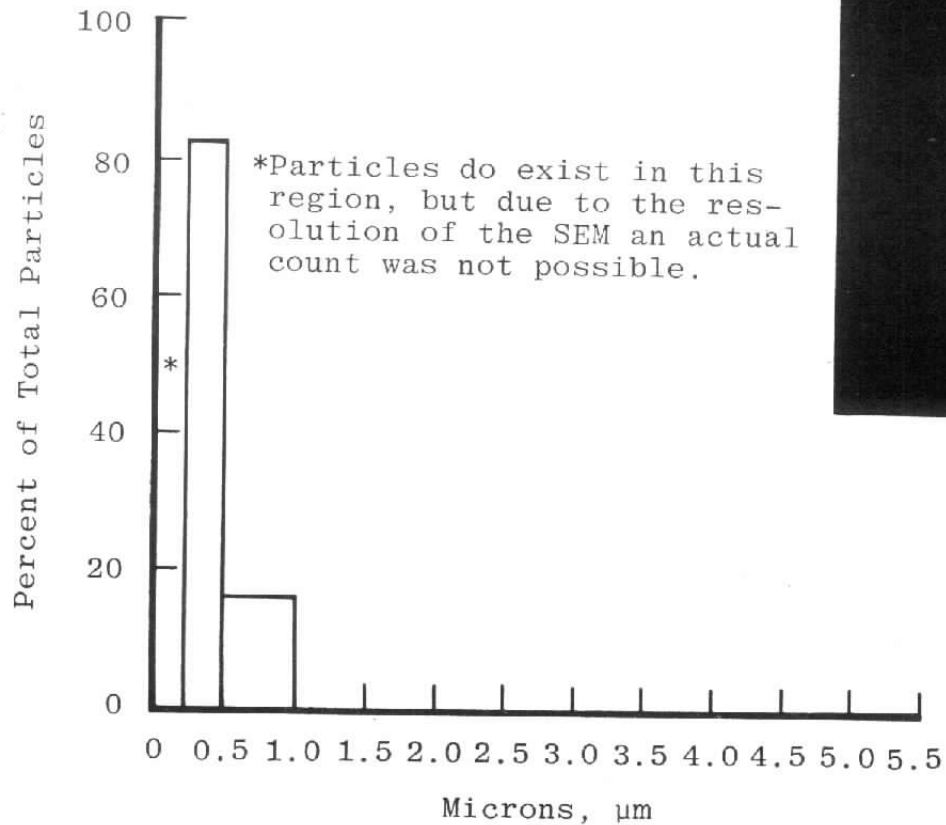
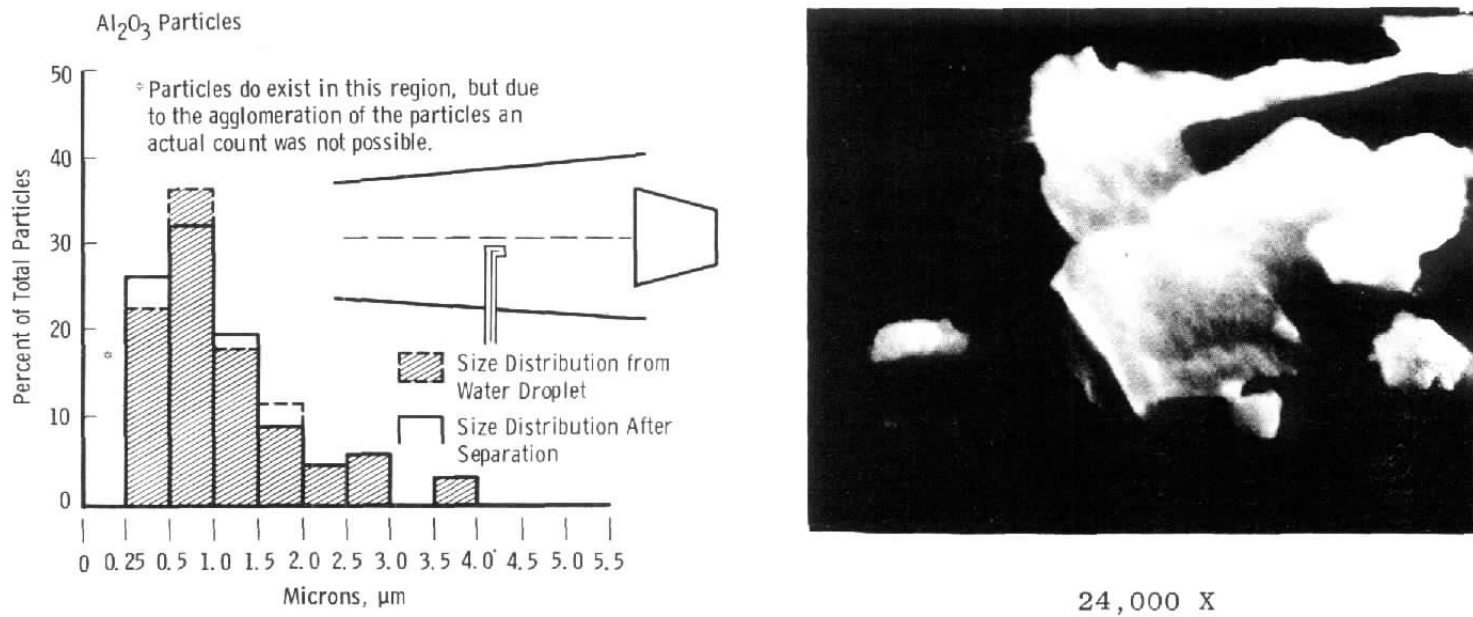


Figure 20. Photograph and histogram of IUS-DS8C tangent probe — Bottle 3 ( $\text{C}_3$ ).



**Figure 21. Photograph and histogram of IUS-DS8C water ingestion probe ( $\text{Al}_2\text{O}_3$ ).**

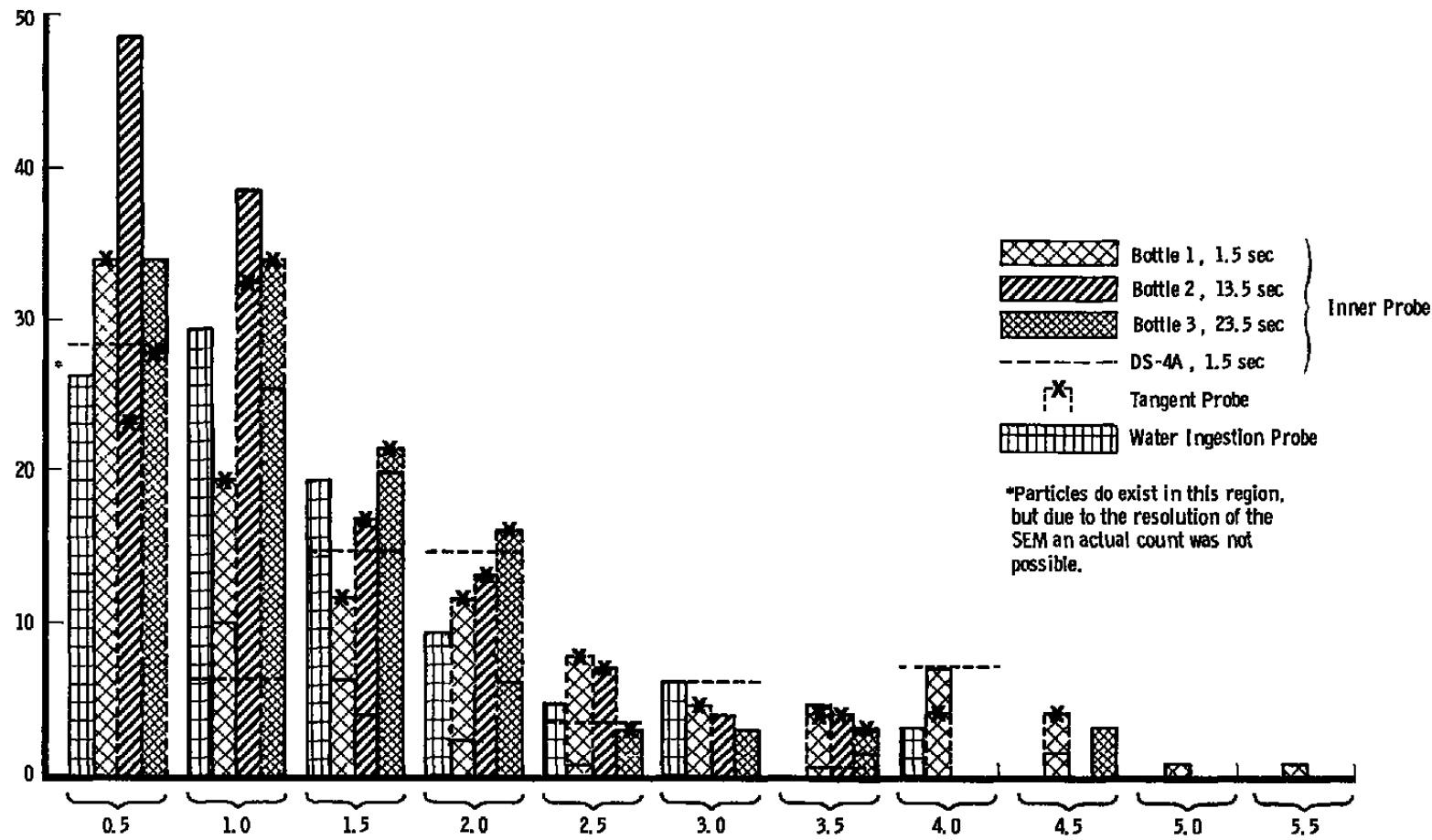


Figure 22. Histogram of all  $\text{Al}_2\text{O}_3$  particles from IUS motors DS-4A and DS-8C.